DEGREE PROJECT

# CFD optimization of photochemical UV reactors for VOC degradation

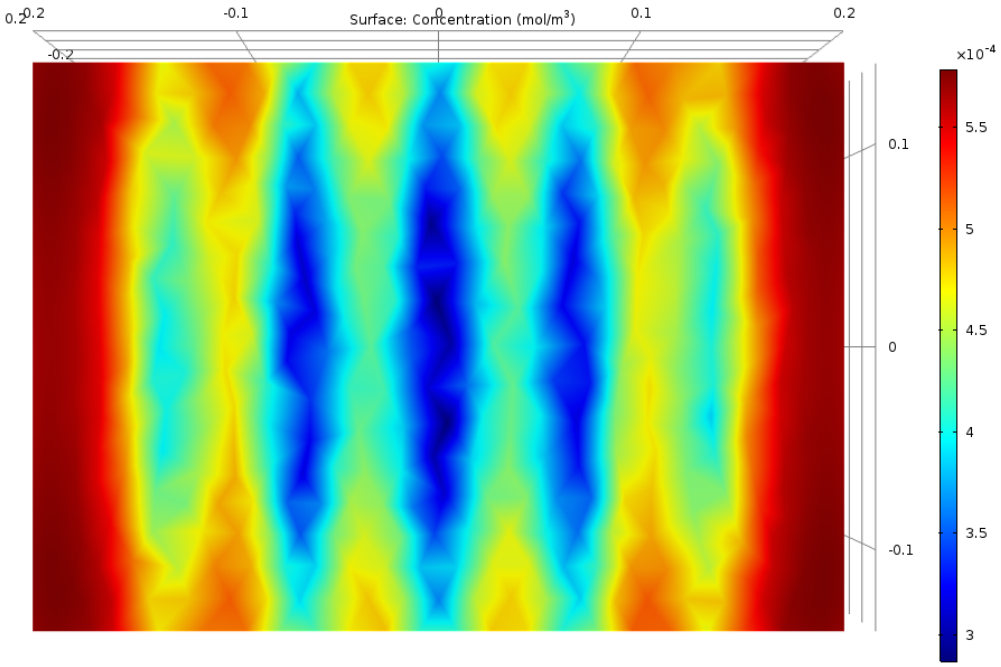


Anna Andersson

**Sustainable Process Engineering, master's level**
**2017**

Luleå University of Technology
Department of Civil, Environmental and Natural Resources Engineering

LULEÅ UNIVERSITY OF TECHNOLOGY

Degree Project

# CFD optimization of photochemical UV reactors for VOC degradation

Anna Andersson

2017

Sustainable Process Engineering, Chemical Engineering
Master's level

Luleå University of Technology
Department of Civil, Environmental and Natural Resources Engineering

# ACKNOWLEDGEMENTS

This thesis was carried out at the Royal Institute of Technology (KTH) in Stockholm, Sweden, in collaboration with Centriair, a company which produces air emission reduction technology. This was my final project before finishing my master's degree in chemical engineering at Luleå Univeristy of Technology (LTU).

First and foremost, I would like to give a big thank you to my supervisor at KTH, Francesco Montecchio, without your knowledge in photochemistry and UV-reactors, your support and your smart ideas this project would not have been as interesting and rewarding as it was. Also, thank you to everyone at Centriair for wanting to investigate if UV-reactors could be optimized. This project would not have been possible without you. A big thank you also goes to Professor Klas Engvall at KTH for always being encouraging and having answers to all problems. I would also like to thank Mireia Altimira for all her help with questions about CFD and PDC. Also, a big thank you to all my other colleagues at KTH for all the fun times and interesting discussions in the lunch room and over fika.

I am also grateful for my supervisor and examiner at LTU, Professor Mattias Grahn. For the quick responses to questions and valuable comments when finalizing this report.

I would also like to give a special thanks to my family, friends and my boyfriend Kristian who all have supported me, given me advice and made this time even better. Thank you!

Also, I wish the reader of this thesis would keep this quote from George Box in mind:

"*All models are wrong but some are useful*" [1]

Stockholm, June 2017

Anna Andersson

# Abstract

In 2016 the World Health Organization released a report on Ambient Air Pollution, in this it was stated that one out of every nine deaths all around the world in 2012 were due to air-pollution-related conditions. Urban air pollution involves a broad range of compounds from many diverse sources. Volatile Organic Compounds (VOCs) are some of the important compounds. Almost all VOCs are known to have effect on human health, many of them are carcinogenic. VOCs also contribute to the ground level photochemical smog and the reduction of the stratospheric ozone layer. Therefore, it is important to control the emissions of VOCs from industries and restaurants.

Today most big scale VOC removal is done by thermal or catalytic incineration. While smaller scale air purification is done by using adsorbing materials such as activated carbon. Both these methods have their drawbacks. A promising technology, which is also environmentally friendly, is UV reactors.

This thesis is a collaboration with the company Centriair, a company developing and selling UV reactors mainly for odor removal. The UV reactors which are in use today work show acceptable performance, with a conversion of 50-60%. However, they have yet to be optimized to get the most out of the reactors. The aim was to try to reach an as high conversion of VOCs as possible in a prototype scale compared to a reference reactor, also in prototype scale. The reactors were simulated using the Computational Fluid Dynamic (CFD) software COMSOL Multiphysics® 5.2a. The simulation was based on earlier lab scale experiments with UV reactors.

The conclusion from doing this thesis is that the most important challenge with a UV reactor up-scaling and optimization is the dark zones and the bypassing effect given by these. It is very important that the irradiation reaches the whole reactor and that all gas is affected by it. It is also important that the gas is given time to stay by the light sources as long as possible. Two reactors in this thesis had very high conversion results and thus showed potential of being very effective UV reactors. One of the most promising reactors has a cubical geometry with a hexagonal lamp configuration with a distance of 8-10 cm between the lamps, together with vortex generators in between the rows of lamps. Also, another configuration is a reactor with short cyclone geometry, where the inner and outer light sources were close to each other, situated near the center of the reactor without being too far from the main fluid stream. These two reactors showed conversion results of 45% respective 61% higher than the reference reactor used by Centriair today.

# SAMMANFATTNING

2016 släppte Världshälsoorganisationen WHO en rapport om luftföroreningar, i denna konstaterades det att ett utav var nionde dödsfall i världen under 2012 var på grund utav luftföroreningsrelaterade betingelser. Luftföroreningar involverar en bred skara av kemiska föreningar från många olika ursprungskällor. Lättflyktiga organiska föreningar (VOCer) är några av de viktiga föreningarna. Det är känt att nästan alla VOCer påverkar människans hälsa, många är dessutom carcinogena. VOCer bidrar även till den marknära fotokemiska smogen och reduktionen av ozonlagret i stratosfären. Alltså är väldigt viktigt att kontrollera utsläppen utav VOCer från industrier och restauranger.

Dagens storskaliga VOC borttagningstekniker bygger på termisk- och katalytisk incineration. Medan tekniken för småskalig luftrening använder adsorptionsmedel, så som aktivt kol. Båda dessa metoder har dock sina nackdelar. En lovande teknik, som även är miljövänlig, är UV-reaktorer.

Denna masteruppstats utförs i samarbete med företaget Centriair, ett företag som utvecklar och säljer UV-reaktorer för främst luktborttagning. UV-reaktorer som används idag visar en acceptabel prestanda, med ett VOC utbyte på runt 50-60%. Dock har dessa reaktorer ännu inte blivit optimerade för att få högsta möjliga utbyte, vilket är målet i detta projekt. Att få ett så högt utbyte som möjligt i en prototyp reaktor jämfört med en referensreaktor, även den i prototyp skala. Reaktorerna är simulerade genom att använda COMSOL Multiphysics® 5.2a, vilket är en programvara för Computational Fluid Dynamic (CFD) simuleringar. Simuleringarna baseras på tidigare försök i labbskala med UV-reaktorer.

Slutsatserna som drogs efter detta arbete var att den viktigaste utmaningen med en uppskalning av UV-reaktorer är de så kallade mörka zonerna, som skapar en bypass i reaktorn. Det är väldigt viktigt att strålningen från ljuskällan når hela reaktorn och att all gas blir påverkad av den. Det är också viktigt att gasen får tid att befinna sig nära ljuskällan så länge som möjligt. Två reaktorer i detta projekt hade väldigt högt utbyte och visar därför stor potential för att bli effektiva UV-reaktorer. En av de mest lovande reaktorerna har en kubisk geometri med lampor som satts i ett hexagonalt mönster med 8-10 cm mellan lamporna, detta tillsammans med virvelgeneratorer mellan raderna av lampor. Den andra konfigurationen är en reaktorn är av kort cyklon typ, där de inre och yttre ljuskällorna är placerade väldigt nära varandra och belägna nära mitten av reaktorn utan att vara för långt ifrån det primära flödet. Dessa två reaktorer visade utbytesresultat på 45% respektive 61% högre än referensreaktorn som Centriair använder idag.

# TABLE OF CONTENTS

# GLOSSARY

| | |
|---|---|
| Amalgam lamp | High end low pressurized mercury lamp. |
| Anthropogenic | Manmade, produced by humans. |
| Biogenic | Produced by living organisms or biological processes. |
| Dark zone | Zone where the polluted fluid gets too little or no irradiation. |
| Envelope | Protective layer around UV-source usually made out of quartz, also called sleeve. |
| Finite line source model | Type of simulation model where the lamp is approximated by a series of spherical light points, located along a line segment |
| k-ε model | Mathematical simplification model for simulation of turbulent flow. |
| Line source | Line of light points located on the lamp, used in line source integration |
| Line Source Integration | Continuous (integral) version of the MPSS technique |
| Mesh | Divides a simulation into small geometries, in every geometry a calculation is made. Smaller mesh means a more detailed simulation calculation. |
| Outlet tube | A tube placed at the outlet of a cyclone, hindering the inlet from flowing straight to the outlet without rotating in a circular motion first. |
| Ozone-free process | UV reactor which does not produce ozone. |
| Ozone-generating | UV reactor which produced ozone |
| Photolysis | When a photon hits a compound and degrades it. |
| Photocatalyst | Catalyst activated by photons from a light source. |
| Photochemistry | Chemical reaction activated by a photon from a light source. |
| Singlet oxygen | Excided oxygen atom or molecule with a high energy level, very reactive. |
| Sleeve | Protective layer around UV-source usually made out of quartz, also called envelope. |
| Turbulence model | Simulation models which simplifies the simulation of turbulent flow. There are several different models to choose from, all of them slightly different for simulations with different needs. |
| $UV/O_3$ | UV process with added ozone, no catalyst. |
| $UV/TiO_2/O_3$ | UV process with both $TiO_2$ photocatalyst and added ozone. |

# ACRONYMS AND NOMENCLATURE

## Acronyms

| | |
|---|---|
| AOP | Advanced oxidation processes |
| CFD | Computational fluid dynamics |
| HAP | Hazardous air pollutant |
| IVL | Swedish Environmental Research Institute |
| KTH | Royal Institute of Technology |
| LPs | Low pressure lamps |
| LSI | Line source integration (a mathematical technique to solve light intensity) |
| LTU | Luleå University of Technology |
| MPs | Medium pressure lamps |
| MPSS | Multiple point source summation (a mathematical technique to solve light intensity) |
| ODC | Ozone decomposition catalyst |
| PCO | Photocatalytic oxidation |
| PDC | Center for high performance computing at the Royal Institute of Technology |
| RANS | Reynolds-average Navier-Stokes |
| UV | Ultra violet, an electromagnetic radiation, 10-400 nm wavelengths |
| UVC | Ultra violet light in the range of 100-280 nm wavelengths |
| VOC | Volatile organic compound |
| WHO | World Health Organization |

## Nomenclature

### Roman uppercase

| | |
|---|---|
| $Abs_{air}$ | Absorption constant · concentration of air [$cm^{-1}$] |
| $Abs_{photon}$ | Absorption of photons in oxygen [$cm^2/mol$] |
| $C_i$ | Concentration of compound i [$mol/m^3$] |
| $C_{O3}$ | Concentration in, $O_3$ [$mol/m^3$] |
| $C_{VOC}$ | Concentration in, VOC [$mol/m^3$] |
| $D_i$ | Diffusion coefficient of specie i [$m^2/s$] |
| $D_{O3}$ | Diffusion coefficient, $O_3$ [$m^2/s$] |
| $D_{VOC}$ | Diffusion coefficient, VOC [$m^2/s$] |
| $Eff_{185}$ | Efficiency of 185 nm irradiation [%] |

| | |
|---|---|
| $Eff_{254}$ | Efficiency of 254 nm irradiation [%] |
| $En_{185}$ | Energy emitted from 185 nm irradiation [J] |
| $En_{254}$ | Energy emitted from 254 nm irradiation [J] |
| F | External forces applied to the fluid [N] |
| H | Height below and above the middle of the lamp [m] |
| I | Identity matrix, mathematical matrix used in linear algebra |
| I | Intensity of the irradiation [$W/m^2$] |
| $I_s$ | Strength of the irradiation [$J^2/s$] |
| $I_E$ | Irradiation, emitted [$W/m^2$] |
| $I_T$ | Irradiation, transmitted [$W/m^2$] |
| L | Lamp length [m] |
| $M_{O3}$ | Molecular weight, ozone [g/mol] |
| $N_A$ | Avogadro's number [$mol^{-1}$] |
| $N_i$ | Flux of specie i [$mol/h \cdot m^2$] |
| P | Time-averaged pressure, the pressure averaged over time [Pa/s] |
| $P_{lamp}$ | Lamp power [W] |
| R | Distance between two light sources [cm] |
| RH | Humidity [%] |
| $R_i$ | Creation and/or destruction of the chemical species, i.e. reaction rate coefficient [$s^{-1}$] |
| $R_{O3\ dec}$ | Reaction rate coefficient for ozone decomposition [$s^{-1}$] |
| $R_{VOC\ dec}$ | Reaction rate coefficient for VOC decomposition [$s^{-1}$] |
| T | Temperature [K] |
| U | Time-averaged velocity, the velocity averaged over time [m/s] |
| $U_f$ | Fluid velocity [m/s] |
| $\dot{V}$ | Volumetric flow rate [$m^3/h$] |

## Roman lowercase

| | |
|---|---|
| a | Distance between the center of the cyclone reactor and the inner lamps [cm] |
| b | Distance between the inner and outer lamps in a cyclone reactor [cm] |
| c | Distance between two outer lamps in a cyclone reactor [cm] |
| h | Distance between the middle of the light source and a point on it [m] |
| k | Turbulence energy in the k-ε model [J/kg] |
| $k_{abs,ozone}$ | Absorption coefficient, ozone [$cm^2/mol$], also called $\sigma_{O3}$ |
| $k_{size}$ | Sizing parameter used in the irradiation calculations |
| $k_{par}$ | Reaction rate constant, VOC decomposition [$m^3/mol$] |
| p | Distance between a point on the light source and a point in the reactor [m] |

| | |
|---|---|
| r | Radius, here of the cyclone reactor [cm] |
| x | Distance between lamp and point n [m] |

## Greek uppercase

| | |
|---|---|
| $\nabla$ | Nabla, a del operator, mathematical operator, denotes the gradient of a vector field in the Navier-Stokes equation |

## Greek lowercase

| | |
|---|---|
| $\varepsilon$ | Epsilon, dissipation rate of the turbulence energy in the k-ε model [J/kg·s] |
| $\mu_T$ | Mu, turbulent viscosity [Pa·s] |
| $\rho$ | Rho, density of fluid [kg/m$^3$] |
| $\rho_{air}$ | Rho, density, air [kg/m$^3$] |
| $\sigma_{O2}$ | Sigma, absorption coefficient, oxygen [cm$^2$/mol] |
| $\sigma_{O3}$ | Sigma, absorption coefficient, ozone [cm$^2$/mol], also called $k_{abs,ozone}$ |

# 1. INTRODUCTION

## 1.1 Background

A recent publication from the World Health Organization (WHO) [2] shows that 92% of the world's population live in areas where air quality levels are exceeding WHO's set limits. WHO continues to state that one out of every nine deaths all around the world in 2012 were due to air-pollution-related conditions. In Sweden, which according to WHO has a good air quality level, the preterm deaths caused by air pollution is approximated to a level of 3500 - 5000 people a year, according to the Swedish Environmental Research Institute (IVL) [3].

Urban air pollution involves several different compounds from many diverse sources, which makes the problem very challenging [4]. Volatile Organic Compounds (VOCs) are some important compounds out of many. Almost all VOCs are known to have effect on human health, many of them are carcinogenic. Also, VOCs contribute to the ground level photochemical smog and the reduction of the stratospheric ozone layer. They come from both biogenic and anthropogenic sources, the majority of the anthropogenic VOCs come from the chemical industry; liquid fuels, solvents, thinners, detergents, degreasers and lubricants etc. [5].

Photochemical smog is formed when UV-light hits oxygen or precursory compounds like VOCs. It is a secondary pollutant; thus the precursory compounds need to be eliminated to be able to hinder the smog formation [4]. Therefore, to solve the air pollution problem, VOC emission needs to be taken care of. Today most large scale VOC removal is carried out by thermal or catalytic incineration [6]. Smaller scale air purification is done by using adsorbing materials such as activated carbon [7]. Both these methods have their drawbacks; Incineration needs high amounts of energy and adsorbing materials remove the pollutant, but it needs to be converted in an additional purification step. Thus, there is a need for an energy efficient and environmentally friendly VOC purification process. The Advanced Oxidation Process (AOP) is a promising alternative, this method utilizes the photons from UV-light to form radicals which in turn will oxidize the pollutants. It is a destructive method which takes care of the VOCs at the source, while not needing any addition of fuel or leading to any $NO_x$ emissions, the only thing needed is the energy in the form of electricity [8].

Today, there are already several UV reactors applying AOP in use around the world. The reactors in these processes operates at a limited performance, usually with a conversion of around 50-60%. However, they have yet to be optimized to get the most out of the reactors. This is the basis of this thesis.

## 1.2 Scope and structure of the work

The aim with this master thesis is to optimize a photochemical UV-reactor, to see if it is possible to increase the conversion of VOCs compared to a reference reactor, also considering the challenges which might occur in the scale up of the process. The project is a collaboration with the company Centriair, a company developing and selling UV reactors mainly for odor removal. Their aim is to develop a system with 98% conversion of VOC, comparing to today's conversion of around 95%. This thesis is part of that research project.

The reactors are based on earlier lab scale UV reactors, where trials had been done to see which parameters influence the VOC decomposition the most. The results where simulated with CFD software, COMSOL Multiphysics® 5.2a which is a reregistered trademark of COMSOL AB, to get a model for reaction kinetics. Knowing the challenges with the existing lab scale reactors a new prototype scale reactor was developed, which was the main task in this master thesis.

The simulations of the reactor were done in steps to be able to compare the different reactors and the problems which were looked into. First the distance between the UV sources was examined, followed by the lamp geometry and the fluid dynamics. These three topics were chosen to be examined as other researchers [9], [10], [11] also had seen problems with UV reactor dark zones, residence time and compounds not getting enough irradiation. A reactor of a more complex geometry, considering the findings found in the optimization, was also simulated. This reactor was optimized as well, to get the most out of the geometry. All the simulations were compared to a reference reactor, similar to a reactor used by Centriair today.

Comparisons were done between the different simulations; discussing how the geometries and lamp placements compare to the reactor used today. Also, discussing the possible issues with scaling up a UV reactor for VOC degradation and if the geometry used today really needs changes or not.

## 1.3 Limitations

This work was limited to looking at the conversion of VOCs in the UV reactors, as increasing the conversion is the main goal of the research project this work is a part of. Any intermediates found in the outlet can be cached by the after-treatment in today's reactor system, thus they were not seen as a major problem at this point.

3D simulations in full scale (with around 15 million units mesh) with only around 5 given equations to solve will take about four weeks to complete on a super computer. Therefore, time was the biggest limitation in this thesis, especially as most simulations in this project involved over 40 given equations. However, by instead doing the simulations with a coarser mesh the time consumption of the simulations

was reduced. On the other hand, the coarser the mesh the less accurate the fluid simulations will be, thus there is a risk that these faster simulations might miss small details. Nonetheless, a few more refined reactors were simulated, showing results in the same magnitude. Thus, it could be assumed that the results in this work are still good indications.

As time was a big limitation, another limitation arises; as with any other simulation project, assumptions need to be taken to be able to calculate the results using an acceptable amount of computational time. This thesis scribes all the assumptions made in the section *3. Method*. For example, in VOC decomposition in field over 100 different VOCs are taken care of in one site. This however, is very difficult to simulate. Therefore, only one common VOC, acetaldehyde, was simulated. Assuming this would represent a model VOC.

Another limitation in this project was the software chosen. There are several different CFD simulation software's available on the market, however only two were available at KTH; ANSYS® FLUENT® and COMSOL Multiphysics® 5.2a. In the beginning of the project the ANSYS® software was used. However, it was soon discovered that the COMSOL® software was a better choice for these simulations, as the needed application were easier to handle in this software. As CFD software's have somewhat different mathematical considerations, it is possible that the results would be slightly different if the simulations were done in some other software.

# 2. Literature Review

The review first takes a glance at what volatile organic compounds are and how they are regulated today in the European Union. A short summary of the VOC removal processes used today and their drawbacks is presented. Then the review goes on with a short history recap on the UV-process, also describing the chemical process behind the UV reactor for VOC abatement. Finally, a more detailed explanation of the UV reactor together with its pre- and after treatments is presented.

## 2.1 Volatile Organic Compounds

According to the European Council directive 1999/13/EC volatile organic compounds or VOCs are defined as:

*"…any organic compound having at 293.15 K a vapour pressure of 0.01 kPa or more, or having a corresponding volatility under the particular conditions of use."* [12]

In other words, a VOC is an organic which has a boiling point under 250 ˚C at standard atmospheric pressure.

VOCs are emitted from both biogenic and anthropogenic sources, a majority of the anthropogenic VOCs come from the chemical industry; degreasers, detergents, liquid fuels, lubricants, thinners and solvents [5]. However, they also come from wood stoves and food processors like the oil for deep-frying as well as from consumer products in indoor environments [13]. Depending on the process, there can be many different VOCs; acids, aldehydes, aromatics, ketones, paraffins, olefins etc. [13]. It is common that there are over 100 different VOCs coming from one industrial process.

VOCs are included in the term *Hazardous Air Pollutant* (HAP), which means that they are in much smaller amount in the atmosphere than the so called Major Air Pollutants, but less is needed for the compound to be hazardous [4]. Almost all VOCs are known to have effect on human health, many of them are toxic and mutagenic [14]. VOCs can also have effects on the human central nervous system. Other than human health they also effect the environment as they are a contributor to the atmospheric pollution process [5]. They promote photochemical reactions in the atmosphere which contributes to the reduction of the stratospheric ozone layer and the formation of secondary pollutants and photochemical smog [14].

## 2.2 Traditional VOC removal methods

There are several types of VOC removal methods in use today. Most of them are good at handling high concentrations of the organics and many of them are effective. However, when it comes to small scale VOC removal, handling low concentrations and not having the space or possibilities to install a big absorption tower or furnace there are not too many traditional options to choose from. Below the most common VOC removal methods are presented.

### 2.2.1 Incineration

At large scale with higher VOC concentrations, most VOC removal is done with thermal or catalytic incineration. Which is the best known methods for disposal of industrial gases [6]. Thermal incineration can have a conversion of 95-99% [14]. However, it needs to be in the temperature range around 750-1150 °C. Catalytic incineration temperature ranges between 200-500 °C [15] with a slightly lower conversion of 90-98% [14]. The heat can be recovered and utilized by producing steam or preheating gas.

If the concentration of VOC is low, additional fuel needs to be added to the process, which will make the incineration process economically unfavorable [16]. Another big disadvantage of this method is the formation of $NO_x$ [16]. Also, problems arise if the combustion does not have enough supply of oxygen, it will then generate partially oxidized compounds which might be even more toxic than the original compound. The catalytic incineration is usually catalyzed by a noble metal on a ceramic support. Usually palladium or platina on an alumina support [16]. However, the combustion products might poison the catalyst, which will give a lower catalytic activity [14].

### 2.2.2 Condensation

Condensation is most efficient for gas streams containing high concentrations of VOCs with a boiling point above 38 °C [14]. If the VOCs have a lower boiling point, better and more expensive cooling or pressurizing systems are needed. The efficiency reaches around 70-85 % [14], however it does not work on all materials, for example materials which might polymerize should be avoided due to the risk of fouling the heat exchanger.

### 2.2.3 Adsorption

Adsorption is divided into two types; physisorption and chemisorption, depending on how the adsorbate and adsorbent interact. Physisorption is when the organic molecule is bonded to the surface of the adsorbent by weak Van der Waals forces. This interaction is reversible and very quick. On the other hand, in chemisorption, strong covalent bonds are formed between the adsorbent and adsorbate [17].

In the adsorption of VOCs, physisorption is the desired process. Traditionally purifying air in smaller scale, with low concentrations, has been done by using adsorbents such as activated carbon or zeolite [7].

However, this technique only transfers contaminants from one place to another, without eliminating them [14]. This means that the contaminants will have to be further processed elsewhere or disposed of together with the adsorption material.

### 2.2.4 Absorption

When using absorption, the VOCs are removed when getting in contact with a liquid solvent in an absorption tower. This technique requires that the VOC is soluble in the solvent. Absorption can have an efficiency of 90-98% [14] if all the VOCs are soluble. However, this removal method, just like adsorption, only moves the VOCs from one fluid to another, thus there is a need to further treat the absorption fluid to dispose the VOCs.

### 2.2.5 Biofiltration

Biofiltration is a quite new and environmentally friendly method for VOC removal. It is mostly used for deodorization [18]. The odorous gas is led through a bed of biologically active material. The microorganisms in the bed oxidizes the VOCs. It requires a low initial investment and has a low operating cost, but the conversion has a very large span of 60-95% [14]. A high conversion requires a mixture of many different microbes, as each is selective to certain VOCs, this however is very difficult to achieve in practice. Also, the conversion largely relies on the residence time in the microbial bed, which normally has to be very high.

## 2.3 The UV-process

Photolysis together with photocatalysis are the main processes of interest occurring in an UV reactor. Already in 1877 it was discovered that sunlight had a negative effect on bacterial growth [19], which was the start of a series of studies leading to the usage of UV-light as a disinfectant method. In 1950 George Porter [20] studied photochemical intermediates by developing a new technology called *flash photolysis*. The continued studies on flash photolysis gave Ronald Norrish, George Porter, and Manfred Eigen the Nobel Prize in Chemistry in 1967 for "*studies of extremely fast chemical reaction, effected by disturbing the equilibrium by means of very short impulses of energy*" [21]. Photocatalytic degradation has been studied since 1970, but it was already mentioned in literature by the Russian Plotnikow in 1910 [22]. In 1970 Fujishima and Honda [23] noted that water can be cleaved by illuminating it with UV-radiation lower than 190 nm over a $TiO_2$ catalyst. At the same time, the concept of photocatalysis was introduced at Institute of Research on the Catalysis and University Claude Bernard in Lyon, France; "*Photocatalyse hétérogène*" [24], [22].

UV irradiation is today the most used physical disinfection process for water purification. In Western Europe many countries use this process as the only disinfection step in the production of drinking water [25]. The concept of UV radiation can also be used for so called *Advanced Oxidation Processes* (AOP),

which is utilized in VOC abatement. When using UV to degrade VOCs there is no risk of formation of $NO_x$ when radiation above 125 nm is used [26] and there is no need for additional fuel. However, there is still a need for added energy in the form of electricity due to the use of UV-lights [16]. Another advantage of the UV-process is that it is conducted at room temperature and at atmospheric pressure [10], which makes it much easier to handle. Commercially today the AOP are mainly used for odor and grease removal [27].

### 2.3.1 The main steps

The removal of VOCs through UV-AOP is composed of three main steps, as seen in Figure (1) below. First the feed needs to be pre-treated to not harm the catalyst or UV-source in the UV reactor. This step mainly takes care of particles and/or sulfur-containing components, which might mechanically wear the UV reactor, stain it or poison the photocatalyst. After the pretreatment, the gas goes into the reactor, where the VOCs will be decomposed. Ozone may be added before the reactor to promote the decomposition of VOCs [28]. The outlet of the UV reactor is composed of air and ozone mixed with the remaining VOCs and some intermediates. The remaining compounds needs to be removed before the air can be released, this is done in the after treatment. This part often consists of activated carbon.

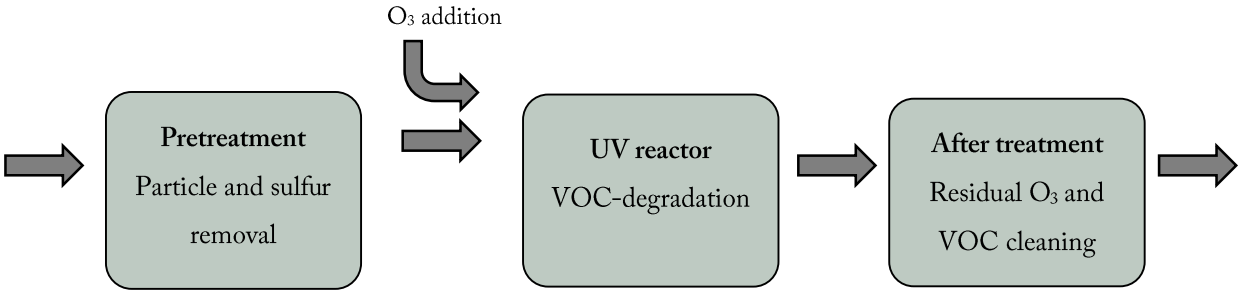


*Figure 1. The main three steps in UV-process for VOC degradation. Depending on the VOC source the steps can be slightly different.*

### 2.3.2 Advanced Oxidation Process

This type of process degrades organic compounds utilizing very reactive and non-selective radicals [29]. In a UV reactor with added ozone, like in Figure 1, the process starts with splitting ozone, oxygen or water in two through so called *Photolysis*, which is when chemical compounds are broken down directly by photons from light, Equation (2.1)-(2.3). If instead ozone is not added, only Equation (2.2) and (2.3) will happen from the start, Equation (2.1) will then occur as soon as ozone is produced, as described in *2.5.6 Ozone*. The molecules have different bonds, thus the photolysis happens at different UV-radiation wavelengths as illustrated in the equations [30], [10], [11].

$$O_3 + hv\ (243 - 310\ nm) \rightarrow\ O(^1D)^\bullet + O_2 \quad (2.1)$$

$$O_2 + hv\ (< 243\ nm) \rightarrow\ O(^1D)^\bullet +\ O(^3P)^\bullet \quad (2.2)$$

$$H_2O + hv\ (175 - 195\ nm) \rightarrow\ OH^\bullet + H^+ \quad (2.3)$$

Where $h\nu$ is the UV-radiation in the specific wavelengths, $^{\bullet}$ denotes that the compound is a radical, ($^1$D) and ($^3$P) is different energy levels of atomic oxygen. ($^3$P) is the ground state, while ($^1$D) is an excited state, it thus has a higher energy level and is therefore more reactive [31]. The newly formed radicals, where OH-radicals are the most important, will then react with the organic pollutant, P, to form a new radical and water, as in Equation (2.4).

$$OH^{\bullet} + P \rightarrow P^{\bullet} + H_2O \tag{2.4}$$

Equation (2.4) can go on repeatedly several times, forming different intermediates if the starting pollutant is a heavy organic compound. However, the organic radical will in the end react with oxygen and be terminated by forming carbon dioxide and water, as in Equation (2.5).

$$P^{\bullet} + O_2 \rightarrow CO_2 + H_2O \tag{2.5}$$

It is possible to summarize the photochemical oxidation process and describe the chemical reaction as Zhao and Yang did [7], seen in Equation (2.6) below.

$$OH^{\bullet} + pollutant + O_2 \rightarrow products\ (CO_2, H_2O\ etc.) \tag{2.6}$$

As the radicals are non-selective they will also react with compounds other than the organic pollutant, in many cases this forms more radicals, which in turn can react with the organic compounds. See the example with a radical reacting with water in Equation (2.7) below. This may happen when there is some amount of humidity in the reactor [11].

$$O(^1D)^{\bullet} + H_2O \rightarrow 2OH^{\bullet} \tag{2.7}$$

## 2.4 Pretreatment

Usually the pretreatment is composed of particle removal and in processes where $H_2S$ might be present; sulfur removal. The particles, which in Centriair's reactors usually is oil mist from frying, is removed down to a size of 1 μm by centrifugal separation. While the $H_2S$ is removed by using a pretreatment reactor filled with α-$Fe_2O_3$ pellets. The interaction between the $H_2S$ and the α-$Fe_2O_3$ cleans the gas from the sulfur by forming iron sulfides or bulk sulfides and water [32].

The pretreatment needs to be done to protect the light source and the catalyst in the UV reactor. Usually the so called *sleeve* or *envelope* around the light source needs to be protected from mechanical wear and from getting dirty. If the sleeve gets contaminated the UV reactor will be less effective as less UV radiation then will reach the reactor. The photocatalyst instead needs to be protected from poisoning e.g. from sulfur by reaction with iron oxides as described above.

## 2.5 UV reactor

UV reactors are comparably simple reactors, there are still many factors to consider when designing a reactor. For example, reaction rate, residence time and flow patterns are important parameters when needing an efficient UV reactor. Experimental results on UV reactors have shown that the reaction rate depends on several different factors, many stated above; photocatalyst characteristics, humidity, reactor type, light source etc. [7]. Below, several of these factors are explained.

The simplest UV reactors are composed of a metallic shell, usually stainless steel. Inside the reactor there are one or several UV-sources, a lamp radiating UV-rays of the desired wavelength, an example with two UV-sources is shown in Figure 2.

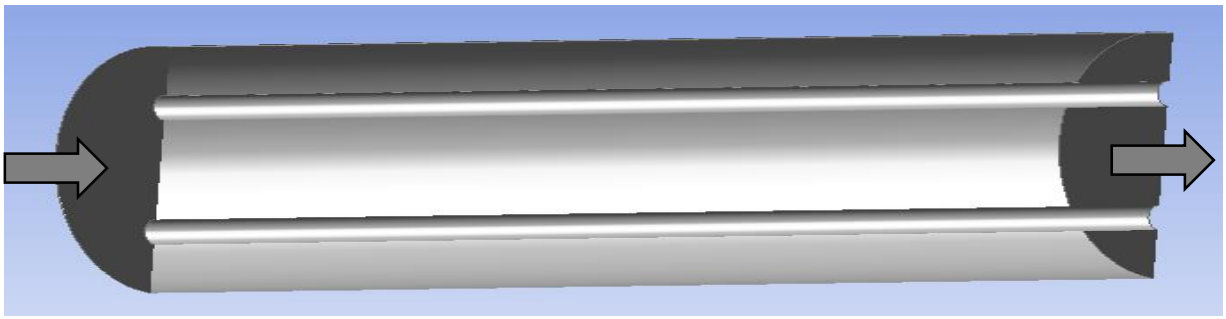

*Figure 2. A cross section of a simple form of UV reactor with two UV-sources (circular light gray rods), where the gas will flow along the light sources, according to the arrows. Inlet to the left and outlet to the right. Figure plotted in ANSYS® FLUENT®. Image use in courtesy of ANSYS, Inc.*

To increase the conversion of the air pollutants an ozone flow can be added to the reactor. This is usually added just before the inlet of the reactor to mix the polluted stream and the ozone before it reaches the UV-source. A photocatalyst can be added on the inside of the reactor, humidity and more UV-sources can also be added and the geometry of the reactor can be optimized, these changes will all promote the conversion of the pollutants. These factors are described more in detail below.

### 2.5.1 Photocatalyst and photocatalysis

A photocatalyst is added to the inside of the UV reactor to catalyze the radical formation. The catalyst is usually made out of a pure or doped semi-conductor [7]. Normally pure titanium dioxide ($TiO_2$) is used as this is cheap, non-toxic, resistant to photo-corrosion and has a high oxidative power. It also has a relatively large band-gap (3.0 eV for rutile and 3.2 eV for anatase [7]) which means that only the UV-radiation with wavelength <380 nm will be absorbed [16]. There are two different crystal structures for titanium dioxide; rutile and anatase. The commercially available catalysts are usually a mix of the two crystals, however, a mix with more anatase is typically preferred as this structure shows superior performance compared to the rutile crystal [7], [33]. However, as studying catalysts are beyond the scope of the present work, the reader can read further on this topic e.g. in *Band alignment of rutile and anatase $TiO_2$* written by Scanlon et al. [33].

Zhang et. al [30] showed that degeneration of toluene using a $O_3/TiO_2/UV$ reactor, was much more efficient than the $O_3/UV$ and $TiO_2/UV$ reactors. Several others [26], [10], [11] have also shown that the usage of a $TiO_2$ photocatalyst is an advantage for reaching a higher conversion of VOCs as the reactions then will be a combination of both photochemical oxidation and photocatalytic oxidation. Therefore, a higher concentration of radicals will form which means that there will be a higher possibility for the organic compounds to encounter radicals and get degraded. However, the photocatalyst will only work if it is first activated by UV-light [34].

In photocatalytic oxidation (PCO) it is important to overcome the band-gap between the valence band and the conduction band. This is done by the formation of electron-hole charge pairs. When the energy, which is provided by the photos from radiation, is greater than the band-gap an electron-hole pair is created [7], Equation (2.8). This charge is then migrating from the pair onto the surface of the catalyst where they react with electron donors and acceptors, Equation (2.9)-(2.11). This is the actual photocatalytic oxidation reaction. The radicals which form will in turn react and form new radicals, Equation (2.12)-(2.13), or degrade VOCs. The charges and OH-radicals are the most important compounds in the photocatalytic degradation of VOCs [7], [16], [11]. The whole process of radical formation using a photocatalyst can be seen in Equation (2.8)-(2.13) below.

$$TiO_2 + hv \rightarrow h^+ + e^- \quad (2.8)$$

$$h^+ + OH^- \rightarrow OH^\bullet \quad (2.9)$$

$$h^+ + H_2O \rightarrow OH^\bullet + H^+ \quad (2.10)$$

$$O_3 + e^- \rightarrow O_3^{\bullet -} \quad (2.11)$$

$$H^+ + O_3^{\bullet -} \rightarrow HO_3^\bullet \quad (2.12)$$

$$HO_3^\bullet \rightarrow O_2 + OH^\bullet \quad (2.13)$$

It is known that doped photocatalyst can give a somewhat higher conversion than conventional $TiO_2$ [35]. However, the doping also means that the catalyst will be more expensive. Montecchio et al. [36] states that P90, which is an undoped $TiO_2$ catalyst, is one of the better alternatives for VOC degradation.

#### 2.5.1.1 Deactivation

In 1981 Cunningham and Hodnett [37] were the first to publish an article describing the deactivation of a photocatalyst. It was then stated that the deactivation of the catalyst during alcohol oxidation was due to the formation of $CO_2$. The $CO_2$ was said to adsorb on the catalyst surface and thus it would compete with the alcohols for the active sites. However, all photocatalytic oxidation processes form $CO_2$ while only some show signs of rapid catalyst deactivation. Therefore, Luo and Ollis [38] instead suggested that the deactivation was due to some less general compounds; certain intermediates. This was also shown in Zhao et al.'s work [7], where intermediates occupied the active sites on the catalyst

and therefore decreased its activity. It was earlier shown in Equation (2.4) that intermediates may form in UV reactors. However, they may degrade completely before the outlet and thus might not always be detected in the outflow of the reactor.

### 2.5.2 Geometry

The geometry of the UV reactor is very important. As the radiation from the UV-source is absorbed by the fluid the number of photons reaching the VOCs will be less further away from the lamp [9]. The amount of photons absorbed by the fluid will depend on the absorption coefficient of the fluid. When using a photocatalyst it is crucial that the photons reach the catalyst, as this will not be activated without the radiation from the UV-light [34].

Many reactors end up having so called *dark zones*, zones where the polluted fluid gets too little or no irradiation to break down the VOCs. These zones will cause a type of bypassing problem, where the polluted gas will go through the reactor without being affected by the irradiation. This problem can according to Wols et al. [9], be avoided if there is enough turbulence in the reactor. Thus, meaning that all parts of the feed will get equal amount of irradiation. Another suggestion is to direct the fluid flow closer to the radiation source with for example baffles. Wols also suggests that the problem can be solved by changing the shape of the reactor or inserting a helix into a cylindrical reactor [9]. Since it is not possible to predict the reactor performance beforehand, it is important to study the dynamics of the flow to identify and mitigate any problems.

### 2.5.3 Light source

The light source is the most important part of a UV reactor. In most cases, mercury UV lamps are used as light source. These lamps are filled with mercury and a so called *starting gas*, usually Argon. There are two main types of these mercury lamps; Low pressure lamps (LPs), which reaches a vapor pressure of 1 Pa, and Medium pressure lamps (MPs) [27]. Medium pressure lamps have a higher electrical power input, this also generates a higher pressure of over 100 kPa. They also have a much higher wall temperature, from 500 to around 950 °C [27]. Compared to LPs the MPs have a much higher UV-flux per unit are length; 35 W/cm compared to 1 W/cm for LPs. However, the life time and efficiency of the UVC is much lower in MPs. Therefore, MPs are mainly just used if the main concern is space efficiency.

Among the low pressure lamps there is a high end version, these are called *Amalgam lamps*. These light sources consist of a mercury mixture (Amalgam means *mixture or blend*), usually a mercury indium combination [27]. This lamp also works with a mercury vapor pressure of 1 Pa, that is reached when the wall temperature is around 100 °C, compared to a standard low pressure lamp which is operated at temperatures around 40 °C. The fact that the wall temperature is higher than a standard LP means that the lamp will be stable at higher temperatures, while a standard LPs will drop in UV output at higher temperatures [27].

Earlier researchers have had problems with short life spans of their amalgam mercury lamps [27], [39]. This was according to Voronov [39] due to formation of HgO on the lamp envelope. As HgO has a very high absorption coefficient in the range of the mercury lamps UV-region, thus it will absorb the radiation. The company Heraeus [39] developed a so called *long life technology*, this consists of a smooth very thin alumina layer. The layer does not absorb or scatter any light. According to Heraeus this technology gives the lamp a service life of 15,000 h with only a 10% efficiency decline, compared to a conventional amalgam lamp without any coating which has a service life of 8,000 h and a 50% efficiency decline [40].

#### 2.5.3.1 Emission spectrum

The advantage of using mercury lamps is due to the emission spectrum these lamps show, they emit two resonance lines with very high efficiency; 254 nm and 185 nm [39]. Radiation between 243-310 nm breaks down ozone through direct photolysis, Equation (2.1). The wavelength around 185 nm is the one responsible for the degradation of water vapor and it is also very effective in producing radicals from air, Equation (2.2)-(2.3). It is also from this wavelength that ozone is produced. Thus, when operating a reactor using a light source with a 185nm wavelength, it might not be necessary to supply ozone [27], this is explained more later. According to Schalk et al. [27] the resonance at 185 nm is mainly applied for advanced oxidation processes, as its direct photolysis will obtain very reactive radicals, according to Equation (2.2) and (2.3).

Chang et al. [11] showed that the combination of 254+185 nm radiation lines over a $TiO_2$ photocatalyst gave a higher ethylene conversion of 45.1% while the usage of 365 nm and 254 nm on their own gave conversions of only 5.14% and 12.1% respectively. Jeong et al. [26] showed a similar result. Jeong also showed that when using the combination 254+185 nm light source in a UV reactor for degrading toluene, the selectivity towards CO and $CO_2$ increased whereas the formation of the intermediate formaldehyde was inhibited. This selectivity is yet another reason for choosing a combined 254+185 nm light source. However, Chang [11] also noted that when using a 254+185 nm light source in humid conditions, secondary organic aerosols will form. Chang proposed that a UV reactor should be operated dry to avoid this, or alternatively an addition of downstream processes should be added to clean the fluid from the aerosols. More on this later under *2.5.7 Humidity*.

#### 2.5.3.2 Residence time

The residence time has to be sufficient for the light to hit the compounds but also for the radicals to react with the VOCs. Both Jeong et al. [10] and Chang et al. [11] showed how the degradation of ethylene decreased with decreasing residence time in the UV reactor. It was then suggested that the conversion would be improved if the residence time was increased. Therefore, according to these results a higher conversion would be given if the residence time was longer.

### 2.5.4 Envelope material

An envelope or sleeve is a material placed around the light source to protect it from contamination. This material is usually quartz or glass. However, not all materials transmit all types of resonance, thus it is an important parameter in a UV reactor. If a softglass (Sodium-Barium-Glass) is used the process will absorb many wavelengths, thus be a so called *ozone-free process*, as softglass does not transmit 185 nm wavelengths [27].

However, if instead fused quartz is used the process can be either *ozone-free* or *ozone-generating*, the highest grade of fused quartz is the very pure synthetic fused silica, which has an outstanding transmittance at all wavelengths of interest [27].

### 2.5.5 Reflective surfaces

Blatchley [25] have looked into the effect of reflecting materials in UV reactors. UV-radiation can reflect of the walls of the reactor and thus lead to photolysis from different angles than just from the UV-source. This is especially important to consider if there are any zones in the reactor where the flow does not get enough radiation from the main UV-source, usually close to walls far away from the UV-source [9]. It has been observed by some researchers that stainless steel has weak ability to reflect UV radiation, less than 20% of the radiation is reflected [25], [41], while polished aluminum reflects about 70% of the radiation. However, in VOC degradation, the air might also contain for example oil mist particles which will contaminate the polished reactor surface and thus leave it with a less reflective surface.

Blatchley [25] tried using mirrors to get more UV-reflection in the process of water disinfection. However, it was shown that polished mirrors show less reflecting characteristics than metal surfaces. Blatchley suggested that it possibly was due to that the reflective surface of the mirror is placed behind a conventional glass, which is known to absorb UV-radiation.

### 2.5.6 Ozone

Ozone is one of the compounds regulated in the European Council directive 2002/3/EC [42]. Ozone is formed by photochemical reactions when UV radiation meets oxygen or precursory pollutants such as $NO_x$ or VOCs [43]. It appears naturally in the stratosphere, 20 to 30 kilometers above the earth's surface. At this altitude, ozone protects earth from the suns UV rays. Still, when found at ground level it can become hazardous [44]. Ozone has a very high oxidizing property, meaning it can be harmful to human health; causing headache, eye, nose and throat irritation and chest pain at levels higher than 214 $\mu g/m^3$ [28]. WHO has set the 8-hour mean limit to 100 $\mu g/m^3$, their research has also shown some evidence that long-term exposure to ozone might have chronic effects [43]. Ozone concentration varies depending on altitude, latitude, season and weather patterns, which is why some countries get the famous *Summer Smog*, linked to the higher temperatures of the region. There are also research showing

that there is less ozone in regions with a lot of car exhaust, as ozone is reduced by NO which is part of car emissions [4].

However, it has been shown that ozone has a positive effect when used to break down the VOCs in UV reactors [28]. As it is regulated it is important that the excess ozone which is not broken down when oxidizing the VOCs is instead removed in the after treatment of the system.

When used in UV reactors, ozone decomposes into unstable radicals with the help of UV radiation, according to Equation (2.1). Combining ozone with a photocatalyst will give an even higher conversion [10], [30], [11]. As the electron affinity of ozone is 2.1 eV and that of $O_2$ is 0.44 eV Pichat et al. [45] states that ozone captures the electrons on the photocatalyst surface easier and will thus form an unstable radical, according to Equation (2.11)-(2.13). For the same reason, Jeong et al. [10] claims that the presence of $TiO_2$ will cause a remarkable reduction in ozone and thus an increase in formation of radicals.

Ozone can both be added by external ozone production as was shown in Figure (1), but it can also be produced by the UV-lamp itself. Jeong et al. [10] states that this formation goes via the following reactions; Starting with Equation (2.2) when the radiation hits an oxygen molecule. The radicals then continue to react with either $O_2$ or $N_2$ until ozone is formed as in Equation (2.15). In a reactor with high air flow it is possible to produce up to 50g/kWh ozone using just the UV-source [39].

$$O_2 + hv\ (< 243\ nm) \rightarrow\ O(^1D)^\bullet +\ O(^3P)^\bullet \tag{2.2}$$

$$O(^1D)^\bullet + \mathrm{M} \rightarrow\ O(^3P)^\bullet + M \tag{2.14}$$

$$O(^3P)^\bullet + M +\ O_2 \rightarrow O_3 + M \tag{2.15}$$

where M is either $O_2$ or $N_2$, which carries the excess energy of the reaction.

### 2.5.7 Humidity

Several researchers [26], [10], [11], [38] have shown that increased humidity gives an increased conversion of VOCs when using $TiO_2$ as photocatalyst. However, Chang et al. [11] showed that this is accurate only when using an UV-source irradiating at wavelengths around 185 nm irradiation. Chang reports that this is due to water molecule being converted into OH-radicals according to the reactions shown in Equation (2.3) and (2.7), where water molecules are turned into OH radicals. These radicals will subsequently react with the VOCs.

Other researchers [46], [47] have shown that some VOCs will experience competitive adsorption from water on a photocatalyst at very high levels of humidity. Cao et al. [47] claims that this is due to that $TiO_2$ is strongly hydrophilic and prefers to adsorb water at higher humidity levels. Furthermore, Cao argues that there is a difference in how sensitive the photocatalysts are to humidity, this depending on their production method.

Jeong et al. [26] and Chang et al. [11] states that secondary organic aerosols are formed when using a 254+185 nm light source. Chang suggests that these form when organic molecules are oxidized, Chang then continues to state that they are compounds with vapor pressure low enough to manage to condense into an aerosol phase. Also, Chang showed that humidity had a substantial role in the formation of the secondary organic aerosols. A high humidity level formed much more aerosols than a low humidity. The ethylene that Chang studied was said to be converted into an acid with low molecular weight, thus it would need a lot of moisture to form aerosols. Therefore, the amount of aerosols formed was higher at high humidity levels. Chang also mentioned that the formation of organic aerosols decreased in the presence of $TiO_2$, however, the reason for this was not stated. It was also noted that if secondary organic aerosols are formed while running a UV reactor they can easily be removed by downstream processes, using existing methods; air filters or wet scrubbers etc.

### 2.5.8 Initial concentration of VOCs

Several researchers [10], [11] have shown that the initial concentration of VOCs is an important parameter when optimizing the conversion in a UV reactor. Chang et al. [11] suggested that a higher concentration of VOCs in the gas will mean that there will be too many molecules to decompose, the radicals will be too few to break them all down, leading to a lower conversion. Therefore, a higher conversion will be the result of a low initial concentration of VOCs.

## 2.6 After treatment

The after treatment in the UV-process can look somewhat different depending on the application of the reactor. Yet, the main purpose of this step is to clean up the residual ozone and VOCs. One method is composed of an ozone decomposition catalyst (ODC) which consists of a manganese dioxide ($MnO_2$) bed, this works well at humidity levels of around 40% and less [26], [10]. At higher humidity levels, over 80%, the ODC is rapidly deactivated. According to Jeong et al. [10] this deactivation is due to adsorption competition between the water and ozone molecules.

There is also another common technique; a bed of activated carbon. Carbon catches both the residual VOCs and ozone. The ozone can then decompose the VOC on the carbon. If the effluent from the UV reactor has a too high concentration of ozone, it will start to make impact on the carbon texture, which might lead to a reduced adsorption capacity of the carbon [48]. As the pores in the carbon might get larger and thus giving a bypassing effect, meaning that some of the gas will flow through the after treatment process faster. Thus, it is always important to know the concentration of ozone in the UV-reactor outlet.

# 3. METHOD

The method section is divided into two large parts; first a short introduction to the software used, followed by a description of the simulations out of a mathematical point of view. The next section continues to describe the optimization; showing the reactors which were simulated in this project.

In this project many simulations were done, first simulations of a simple cubical reactor were done, as this geometry is similar to the reactors used by Centriair today. After doing the literature review it was decided to focus on the so called dark zones as this was noted to be an important problem in many UV reactors. Thus, effort was put on getting as much gas as possible to reach the zone where the UV-radiation is most efficient, close to the light source, also to increase the residence time of the gas close to the lamps. Three important features which could be optimized to solve this was chosen; distance between lamps, lamp geometry and fluid dynamics. Later some simulations on a more complex geometry were also performed, this still having similar considerations.

All of these trials could have been done as ordinary experiments in lab- or prototype scale, however the approach with simulations was chosen as it is both too expensive and time consuming to do all trials as real experiments. CFD simulations were used as this problem area revolves around the fluid flow. Assuming that the chemical reactions in the simulation corresponds to the ones in the experiments made earlier in lab-scale, it is possible to optimize a reactor by using simulations. Simulations do however not replace experiments fully, which is why the reactors also should be tested in the field, to verify if the simulations in fact correspond to reality.

To save computational time several simulations were done using the super computer *Tegner* at the Center for high performance computing at the Royal Institute of Technology in Sweden (PDC), more information about the Tegner hardware can be found on the PDC website [49]. The simulations not performed on Tegner were instead performed on a stationary computer with an Intel® Core ™ i7-4790 CPU at 3.60 GHz with a 16.0 GB RAM.

## 3.1 Computational Fluid Dynamic simulations

The best way of studying the mixing behavior in a UV reactor is by using turbulence models, like Computational Fluid Dynamic (CFD) simulations [50]. The simulations which were carried out in this work were done in the CFD software COMSOL Multiphysics® 5.2a. Some numerical calculations were also performed using the software MATLAB® R2015b. To simplify the modelling, several simplifying assumptions were considered while doing the calculations. This Method section will describe the equations used and the assumptions stated during the simulations.

To minimize the number of changeable parameters, some were set constant for all the simulations, see Table 1:

*Table 1. The constants used in all the COMSOL Multiphysics® 5.2a simulations.*

| Parameter | Abbreviation | Value |
|---|---|---|
| **Humidity** | RH | 80% |
| **Temperature** | T | 313.15 K (40 °C) |
| **Volumetric flow rate** | $\dot{V}$ | 100 $m^3/h$ |
| **Absorption constant, air** | $Abs_{air}$ | 4.92 /m |
| **Absorption constant, $O_3$** | $\sigma_{O3}$ / $k_{abs\ ozone}$ | 7.05e6 $cm^2/mol$ |
| **Reaction rate constant, VOC decomposition** | $k_{par}$ | 50000 $m^3/mol$ |
| **Lamp power** | $P_{lamp}$ | 10 W |
| **Lamp length** | L | 0.28 m |
| **Concentration VOC, in** | $C_{VOC\ in}$ | 6.1e-4 $mol/m^3$ |
| **Concentration $O_3$, in** | $C_{O3\ in}$ | 0 $mol/m^3$ |

It was decided to keep the number of changeable parameters as low as possible to be able to compare the different reactors, both the simulations and also in field trials (not included in this thesis). When testing the reactors in field, it would be very hard to get the exact same amount of catalyst loading in each reactor, as this depend a lot on the geometry of the reactor. Also, a photocatalyst would mean several more equations to solve for every simulation, as this thesis is the first step in optimizing a UV reactor using CFD simulations it is important to not make the simulation too complicated from the start. Thus, it was decided to exclude the photocatalyst out of the simulations.

The same was decided regarding the ozone, no ozone should be added to the feed in the simulations. This due to, as stated above, the need of having as few changeable parameters as possible and keeping the simulation simple. However, the reactors are all generating ozone. Thus, there will still be ozone present in the reactors, as described in the Literature Review.

Further, the humidity was fixed to 80%. It was then also assumed to only be taken into consideration in the kinetic constant. As earlier stated the humidity will affect the conversion of the VOCs. However, to keep the parameters down to a minimum, it was decided to not focus on this in this thesis.

The reactors were all simulated in stainless steel, as stated in the Literature Review this material only has a 20% reflection compared to polished aluminum with around 70% [25], [41]. In a brand new stainless steel reactor this will have a small effect on the conversion, as the irradiation will reflect of the walls of the reactor and thus come from different angles. If the reactors instead were built in aluminum there would be a larger effect on the conversion. However, generally aluminum is more expensive than

stainless steel [51]. This together with the fact that the reflection will decrease over time, due to dirt, it is in many cases not worth building the reactors in aluminum.

### 3.1.1 Irradiation

The light emission was calculated according to a technique called *Multiple Point Source Summation* (MPSS), which means that the irradiation from the lamp is assumed to be *m* number of point sources, all spaced equally along the lamp axis [25], [50]. More specifically, in a *Finite line source model* the lamp is approximated by a series of spherical light points, located along a line segment on the lamp [52]. All the points in the reactor is then exposed to light from all points on the line. When using this model a continuous version of the MPSS technique can be used, called *Line Source Integration* (LSI) [41].

The points were calculated in every point n at distance x from the lamp, height H above and below the center of the lamp of length L, as seen in Figure 3.

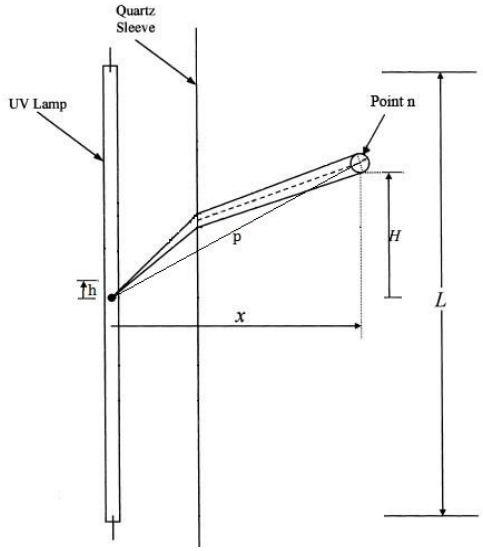


*Figure 3. Schematic illustration of the Finite line source model. L is the length of the lamp, x is the distance between the lamp and point n, H is the height of the point from the middle of the lamp, p is the distance between the point on the light source and the point in the reactor and h is the distance between the middle of the light source and the point on it. Figure redesigned from Bolton [41].*

The distance, p, between point n and a point on the light source is given by Pythagorean theorem. As seen below in Equation (3.1)

$$p^2 = (H - h)^2 + x^2 \tag{3.1}$$

Where h is the distance between the middle of the light source and the point on the light source. The irradiation from one point of light is given by Lambert's law of absorption [53], as seen in Equation (3.2) below.

$$\frac{1}{(p^2)} \frac{d(p^2 I)}{dp} = -\sigma I \tag{3.2}$$

Where I is the intensity of the irradiation and σ is the absorbance of the fluid.

Equation (3.2) integrates to the following expression.

$$I = \frac{I_S\, dh}{4\,\pi\, p^2} e^{-\sigma p} \tag{3.3}$$

Where $I_s$ is the strength of the line source. Since Equation (3.3) cannot be integrated analytically [53], the absorption expression is neglected together with the reflection and refraction [41], [25], giving the following Equation (3.4).

$$I_E = \frac{I_S\, dh}{4\,\pi\, p^2} \tag{3.4}$$

When assuming no absorption, reflection or refraction, it is possible to obtain an integral form of the equation, shown below. Here $I_s$ is also substituted with the lamp power, $P_{lamp}$, and the efficiency, $Eff_{irradiation}$.

$$I_E = \int_{-L/2}^{L/2} \frac{P_{lamp}\, Eff_{irradiation}\, dh}{4\,\pi\,(x^2+(H-h)^2)} = \frac{P_{lamp}\, Eff_{irradiation}}{4\,\pi} \int_{-L/2}^{L/2} \frac{1}{(x^2+(H-h)^2)}\, dh \tag{3.5}$$

The resulting equation is the one used for the simulations in the COMSOL® software. The integration corresponds to taking the number of points, m, to infinity.

$$I_E = \frac{P_{lamp}\, Eff_{irradiation}}{4\,\pi\, L\, x} \left[\arctan\left(\frac{L/2+H}{x}\right) + \arctan\left(\frac{L/2-H}{x}\right)\right] \tag{3.6}$$

The reactors in this project are simulated in stainless steel, thus the reflection from the walls should be less than 20% as earlier stated. The reflection would be even less significant when the reactor has been in operation for some time, due to eventual particle deposits. Therefore, the reflection was set to zero. The gas absorption however affects the conversion to a much larger extent, as it affects both the ozone production and the VOC degradation. This was considered too important to neglect, thus this was incorporated into the transmitted radiation, described below.

The radiation from the lamp which hits the VOCs at different distances from the light source is described by the transmitted radiation, $I_T$. Which is given by Beer-Lambert's law, where the radiation emitted from the light, $I_E$, given by Equation (3.7) below. The radiation with a wavelength of 185 nm was assumed to only be absorbed by oxygen in the air, as this wavelength does not affect nitrogen, thus for this wavelength the Beer-Lambert's law can be written as in Equation (3.7).

$$I_{T\,185\,nm} = I_E\, e^{-\sigma_{O2}\, C_{O2}\, x} \tag{3.7}$$

As the concentration of $O_2$ is approximately constant in air, only small amounts are decomposed to form ozone (ppm levels) and sigma is also constant, these two can thus be combined into; $\sigma_{O2}\, C_{O2} = Abs_{air}$ (absorption air). Yielding:

$$I_{T\,185\,nm} = I_E\, e^{-Abs_{air}\, x} \tag{3.8}$$

The radiation at a wavelength of 254 nm is instead absorbed by the ozone produced. However, the concentration of ozone is not constant. Therefore, this equation cannot be simplified, instead it was used as it is, as in Equation (3.9) below.

$$I_{T\,254\,nm} = I_E\, e^{-\sigma_{O3}\, C_{O3}\, x} \tag{3.9}$$

However, as the emitted light, $I_E$, was calculated with the assumption that there would not be any absorption there will be a slight difference between the simulated results and reality. Thus a sizing parameter is added to the simulations. The calculation for the sizing parameter is based on the difference between the simplified Equation (3.8) and (3.9) and the more complex Equation (3.10), which is a rewritten version of Equation (3.3), solved numerically.

$$I_T = \int_{H\,min}^{H\,max} \left( \frac{P_{lamp}}{4\,\pi\,L} \left[ \left( \frac{1}{H+\frac{L}{2}} \right)^2 + x^2 - \left( \frac{1}{\frac{L}{2}-H} \right)^2 + x^2 \right] e^{-Abs_{Air} \sqrt{\left( \frac{1}{H+\frac{L}{2}} \right)^2 + x^2 - \left( \frac{1}{\frac{L}{2}-H} \right)^2 + x^2}} \right) \tag{3.10}$$

The aim of the calculation was to find a sizing parameter which makes the difference between the two calculation cases as small as possible. This sizing parameter, $k_{size}$, was calculated for each reactor as it changes with the reactor geometry, this was done using MATLAB® R2015b. The result was then put into the equations in the COMSOL® software as a constant. Thus, the equations used in the COMSOL® simulations for the calculations for transmitted irradiation are the following:

$$I_{T\,185\,nm} = I_E\, e^{-Abs_{air}\, x\, k_{size}} \tag{3.11}$$

$$I_{T\,254\,nm} = I_E\, e^{-\sigma\, C_{O3}\, x\, k_{size}} \tag{3.12}$$

Jacob and Dranoff [53] showed that the difference between the calculated and experimental intensities when using this approach were of the same order of magnitude. However, in their trials, where a cylindrical reactor was used, it was also observed that it was important to take note when increasing the radius of the reactor. As the reactor volume will increase with the square of the radius. Also, the outer parts of the reactor contribute greatly to the overall conversion. Therefore, small differences in this region might affect the predicted performance significantly.

### 3.1.2 Reactive models

Several chemical reactions are very difficult to simulate at the same time, due to the case complexity. Therefore, it is usually assumed that one or a few compounds is a model of the whole group of species. In this project it was assumed that acetaldehyde would represent the model VOC, as it is often found in industrial air emissions. The reaction rate constant for the decomposition of acetaldehyde was obtained from the earlier lab scale trials, it can be seen in Table 1 as $k_{par}$.

Below are descriptions of first the ozone formation and then the degradation of both ozone and VOCs.

#### 3.1.2.1 Ozone formation

As stated earlier the concentration of ozone is not constant. The generation of ozone by the UV-lamp was assumed to be the only source of ozone, i.e. assuming no added ozone or other ozone in the inlet gas. For every photon absorbed in oxygen, $Abs_{photon}$, it was assumed that two ozone molecules would form, according to Equation (3.13).

$$O_{3\ generation} = \frac{2\ Abs_{photon}}{N_A} \tag{3.13}$$

Where $N_A$ is Avogadro's number. As oxygen only takes up radiation with wavelength of 185 nm, the absorption of photons can be expressed as the absorption of the 185 nm radiation, $Abs_{185}$, divided by the energy emitted from the same radiation, $En_{185}$.

$$Abs_{photon} = \frac{Abs_{185}}{En_{185}} \tag{3.14}$$

The absorbed radiation is in turn expressed as the emitted radiation minus the transmitted radiation of oxygen.

$$Abs_{185} = I_E - I_{T\ 185\ nm} \tag{3.15}$$

Where both $I_E$ and $I_T$ are expressed in Equation (3.6) respective Equation (3.11) above.

#### 3.1.2.2 Decomposition of ozone and VOCs

It was assumed that the reaction rate for the decomposition of the ozone was directly proportional to the concentration of OH-radicals in the reactor. This in turn can be assumed to be proportional to the reaction rate of the decomposition of the VOCs, if all radicals are used to decompose VOCs. As seen in Equation (3.16) below:

$$R_{O3\ dec} \propto [OH^{\bullet}] \propto R_{VOC\ dec} \tag{3.16}$$

This would mean that the decomposition of ozone only forms OH-radicals and that only OH-radicals are breaking down the VOCs i.e. there are no other radicals present in the reactor. In reality this will not be the case. Thus the simulation will underestimate the radical count, however, together with an overestimation of the VOC degradation, as only one type of VOC is used, this assumption was deemed to be feasible.

This, in turn, means that the decomposition of ozone can be used to describe the decomposition of the VOCs. The reaction rate of the VOC decomposition is based on the concentration of VOC and OH-radicals, but as the OH-radicals is proportional to the reaction rate of ozone decomposition, this can be used instead, as seen in Equation (3.17).

$$R_{VOC\ dec} = k_{par}\ [VOC]\ [OH^{\bullet}] = k_{par}\ [VOC]\ R_{O3\ dec} \tag{3.17}$$

The decomposition of ozone was assumed to be due to only photolysis, as no photocatalyst was used. Thus the reaction rate would be proportional to the irradiation absorbed by the ozone; the emitted radiation minus the transmitted radiation as in Equation (3.18).

$$R_{O3\ dec} \propto I_E - I_{T\ 254\ nm} \tag{3.18}$$

As the transmitted irradiation affecting ozone is expressed according to Equation (3.12), then Equation (3.18) can be rewritten as below.

$$R_{O3\ dec} \propto I_E - I_E\ e^{-\sigma\ C_{O3}\ x\ k_{size}} = I_E\ (1 - e^{-\sigma\ C_{O3}\ x\ k_{size}}) \tag{3.19}$$

From this it is now also possible to rewrite the reaction rate of VOC decomposition, Equation (3.17).

$$R_{VOC\ dec} = k_{par}\ [VOC]\ (I_E\ (1 - e^{-\sigma\ C_{O3}\ x})) \tag{3.20}$$

### 3.1.5 Turbulent flow, k-ε model

A laminar flow is very predictable while turbulence is a very complicated phenomenon [54]. When a turbulent flow moves along a geometry like a flat plate, as seen in Figure 4 below, several different layers will form; Turbulent region, buffer zone and viscous sublayer. As all these regions behave differently it makes a turbulent flow harder to simulate.

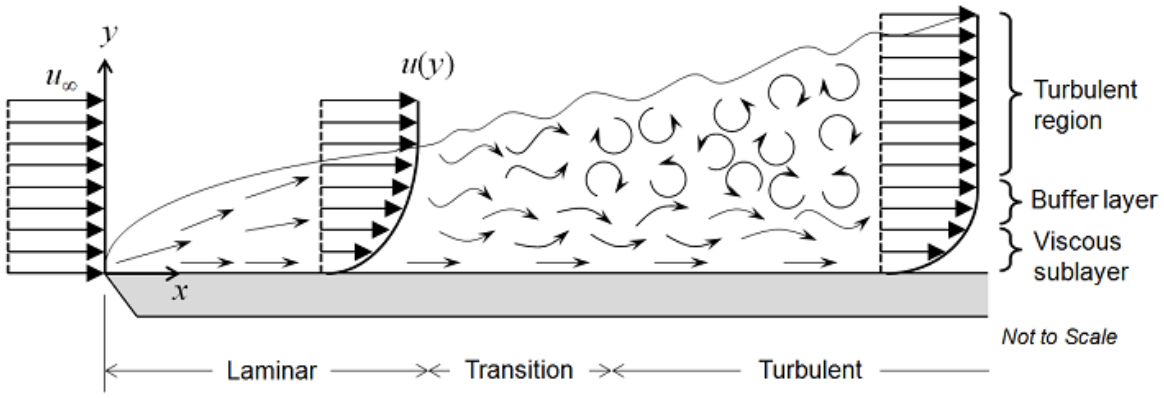


*Figure 4. The three different regions of flow and the layers of the turbulent region. Image credit: COMSOL [55]*

Exact turbulent flows are hardly ever simulated. This is due to the complexity of them, a real turbulent flow consists of eddies down to the size of millimeters. Simulations can stretch to meters or even kilometers. This amount of calculations would demand a computer with huge amount of storage and also large amounts of time [56]. Therefore, there is a need for simplified models, so called *turbulence models*. There are several different simplification-models, in this project the *k-ε model* was chosen, which is a very robust model with a reasonable computational time [57].

The k-ε model breaks down the turbulent flow into two differential equations; turbulence energy, k, and the dissipation rate of the turbulence energy, ε. The model also emphasizes on the flows nearby the solid

walls of the simulated geometry. At the wall there will be a local Reynolds number which is very small, this means that the viscous effects will dominate over the turbulent in these areas [56], as in the viscous sublayer in Figure 4. Therefore, this region need to be treated differently mathematically. In this project this is solved with the so called *Enhanced wall treatment*. This is when the solver treats everything up until a distance of a point P from the wall as the same viscous flow, assuming an analytical solution for the flow in this layer. This layer would in reality have zero velocity by the wall and gradually having a higher and higher flow rate. After point P the viscous effects are assumed to be entirely taken over by the turbulent effects. Thus, the buffer zone between these areas is assumed non-existent [55].

The motion of a Newtonian viscous fluid can be calculated using the Navier-Stokes equation [54]. However, to save computational time when simulating a turbulent flow, a Reynolds-averaged Navier-Stokes (RANS) equation can be used instead [57]. In this equation the velocity and pressure fields are time-averaged. The RANS equation is shown in Equation (3.21) below.

$$\rho(U \cdot \nabla U) + \nabla \cdot \left(\mu_T(\nabla U + (\nabla U)^T) - \frac{2}{3}\mu_T(\nabla \cdot U)I\right) = -\nabla P + \nabla \cdot \left(\mu(\nabla U + (\nabla U)^T) - \frac{2}{3}\mu(\nabla \cdot U)I\right) + F \quad (3.21)$$

where U and P are the time-averaged velocity and pressure, ρ is the density, ∇ the del operator, I is the identity matrix, F is the external forces applied to the fluid and $\mu_T$ the turbulent viscosity. $\mu_T$ is evaluated using a turbulence model, this is described further below.

The Navier-Stokes equation represents the conservation of momentum, as the conservation of mass is also needed the Navier-Stokes equation will always be solved together with the Continuity equation, Equation (3.22).

$$\rho\nabla \cdot U = 0 \quad (3.22)$$

In this project, the fluid was assumed to be only slightly compressible, thus it is assumed that the density and the temperature of the fluid will not change [57]. This also means that there would be no need to solve the energy equation, only the above Equation (3.21) and (3.22).

### 3.1.6 Transport of diluted species

The concentration of VOCs in the reactor in this project was, as in most applications, very low, with an inlet concentration of 6.1e-4 mol/m$^3$. Also, with no added and only small amounts of ozone formed it was necessary to use the physical model called *Transport of Diluted Species* when simulating the transportation of both the VOC and ozone.

When having a fluid in motion advection will occur and the concentration gradients in a fluid will in turn cause mass transfer by diffusion. Thus there is often a need to solve for a combination of the two [58], this is usually done according to the Advection-Diffusion equation seen in Equation (3.23).

$$\frac{\partial c_i}{\partial t} + \nabla \cdot N_i = R_i \quad (3.23)$$

Where $\frac{\partial C_i}{\partial t}$ is the concentrations of the specie i over time and $R_i$ describes the creation and/or destruction of the chemical species, i.e. the reaction rate. When simulating a reacting system with a fluid flow, the specie i's flux, $N_i$, is expressed as the diffusion (Fick's first law of diffusion) combined with the advection [59] according to Equation (3.24) below.

$$N_i = -D_i \nabla c_i + C_i U_f \tag{3.24}$$

where $D_i$ is the diffusion coefficient and $C_i$ is the concentration for each specie, $U_f$ is the fluid velocity.

## 3.2 Optimization

Several different reactor configurations were simulated with the aim of increasing the conversion. The reactor used by Centriair today was also scaled down and simulated in prototype scale (40x40x28 cm) to be able to compare the results. The optimization was done by simulating simple cubical reactors of continuous type focusing mainly on the three problem areas; lamp distance, lamp geometry and turbulence. If nothing else is stated, all reactors have a fluid flow along the x-axis, with an inlet shown to the left in the geometry figure and an outlet on the opposite side, to the right in the figure. The gray colored part of the figure is where the fluid will flow in the simulation, while the holes are where there is a solid object, such as a lamp source.

### 3.2.1 Reference reactor

In Figure 5 below, the reactor geometry of the scaled down reference reactor is shown together with the axis coordinates and arrows showing the gas flow along the x-axis. The axis is the same for all of the following reactors in this report.

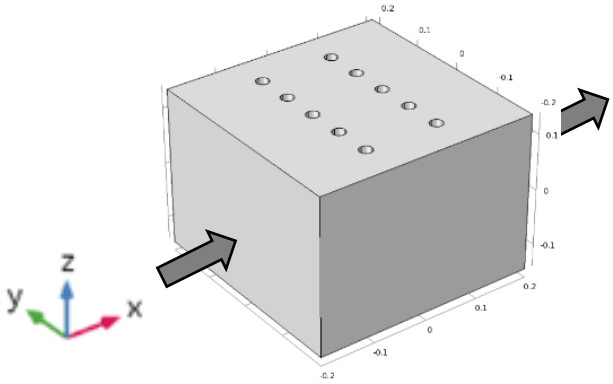


*Figure 5. The geometry of the reference reactor which is used by Centriair today, Case 1. Also showing the axis, which is the same in all the following geometries.*

This reference reactor is a simple cubical reactor which has the light sources in two rows straight after each other. The light sources consist of low pressure mercury lamps within quartz sleeves. This reactor will further be referred to as Case 1 or the reference reactor.

### 3.2.2 Lamp distance and geometry

First the distance between the light sources was tested to see if this distance has any effect on the conversion. This was done using lamp sources placed in a hexagonal pattern. This specific pattern was chosen as it gives the chance of having all lights at the same distance to each other. The distance between the lights, R, was changed for every simulation. The distance between the light source and the wall was also fixed to be R/2, as this means that the irradiation distance needs to be the same between the lights as between a light and the wall. As all the distances change, the reactor size will also change for each simulation. The simulations were done when R equals 5 and 9 cm and 6-20 cm, with steps of 2 cm. Thus, giving a total of ten simulations. Three of them are seen in Figure 6 below.

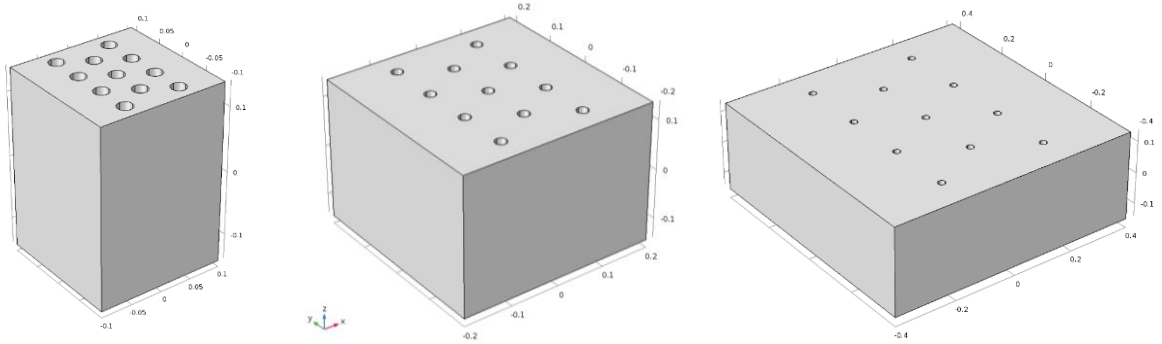

*Figure 6. The geometry of reactors with light sources placed in a hexagonal pattern. This rector configuration was used to test the distance between the lamps. Here showing from the left; Case 4a, 4e and 4j, with R=5, 10 and 20 cm.*

Different lamp geometries were also tested. This means that the lamps were placed in different configurations to see if it affected the conversion in the reactor. Below in Figure 7 the six of the seven different cases of geometries are shown, however, two of them look the same but have different flow directions. The last case has the same geometry as case 4e in Figure 6 above.

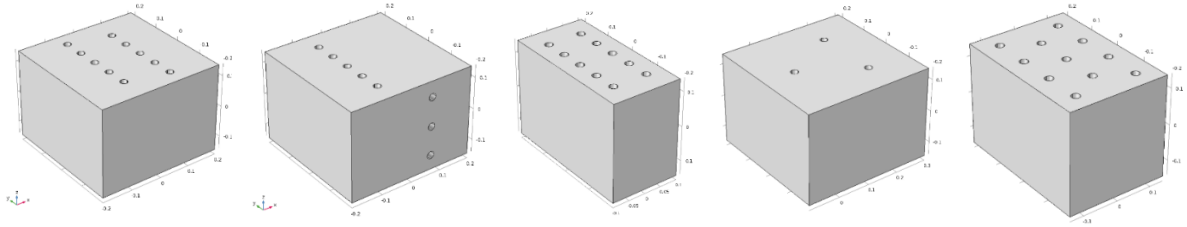

*Figure 7. Different lamp configurations. These were used to test if the placement of the lamp had an effect on the conversion. Here showing, from the left; Case 3, 5, 6, 7, 8 and 9, where the last two look the same but have different flow directions.*

The seven cases were compared to the reference reactor. Case 6 and 8 have their inlets and outlets placed with the flow going along the y-axis, i.e. the inlets are placed at the back left side of the geometry figure and outlets on the opposite side, which is shaded in the figures. Case 9 on the other hand has its flow going along the z-axis, meaning that the inlet is on top of the reactor and outlet at the bottom, thus in this reactor the gas flows along the length of the light sources.

### 3.2.3 Fluid dynamics

One way of letting the gas mix while also making it stay close by the light source for a longer time is by adding vortex generators. Vortex generators are triangular shaped rods fitted into the reactor to form more vortexes, thus improving mixing. In this project it was decided to place them perpendicular to the light sources, as this was assumed to be the best way of breaking the stream lines. These reactors with vortex generators were compared to the simulations with lamps placed in the same configuration, of same size, but without the generators. In Figure 8 below the five simulation geometries are shown.

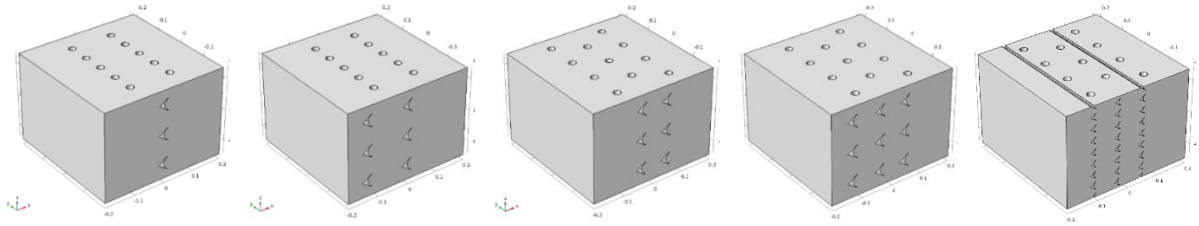

*Figure 8. The different cases with vortex generators, used to test what effect turbulence has on the conversion. Here showing, from the left; Case 10a, 10b, 11a, 11b and 11c.*

## 3.3 Complex geometry

It was decided that a few reactors with more complex geometries should also be evaluated. Thus, a cyclone type of reactor was simulated. This geometry was chosen as it will allow the gas to flow pass the lights several times i.e. it will have a long residence time close to the lamps, while also facilitating good mixing. The circular motion was thought to be enough to give a homogenous irradiation of the polluted gas. The geometry is round and the flow would follow a typical cyclone stream. That is, flow clockwise on the outside of the lamps and then change direction when reaching the middle in the bottom, shifting for a counter clockwise motion on the inside of the lamps towards the outlet at the top of the reactor. Thus, it was also assumed that there would not be any zones were the irradiation would not reach or where the gas could go by without getting any radiation.

Many researchers have investigated cyclone reactors with the aim of optimizing the performance. However, to the best of our knowledge no one has studied the use of a cyclone configuration for a UV reactor. As this application is very different from the normal usage of cyclones it is not possible to look only at earlier cyclone work. The best is to just simulate what works for this application.

The simulations of the complex geometry were also divided into three areas; Geometry, outlet and lamp distance.

### 3.3.1 Reactor geometry

First the reactor geometry was evaluated, simulating two different geometries; One of traditional cyclone shape, case A, and another one smoother more conical one in case B. These two were then made wider

at the bottom. Case B was also made shorter together with moving all the inner lights up to the top part of the reactor, creating case C. All of the changes were mainly done to see if it made the fluid flow more stable around the lights. A stable flow would mean more circular movements and thus also a longer residence time in the reactor. All of the geometries are shown in Figure 9 below.

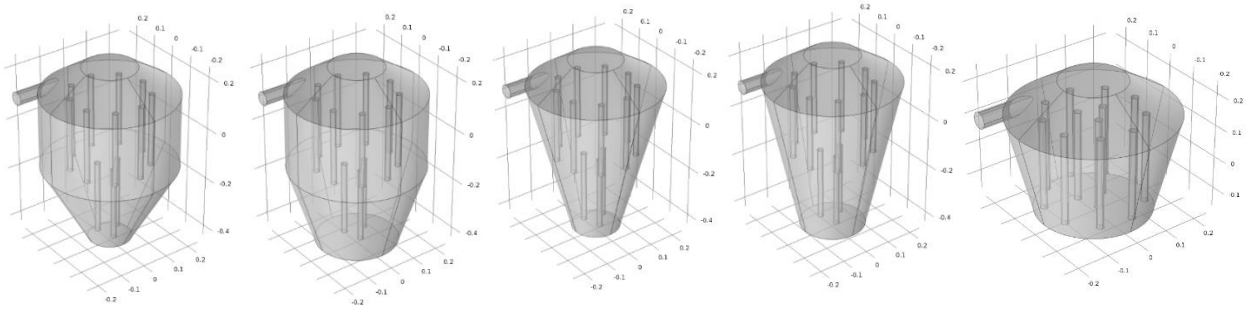

*Figure 9. The five cyclone geometries evaluated. From the top left; case A1 and A2, where A2 has a somewhat wider bottom. Bottom left; case B1, B2 and C, where B2 has a wider bottom and C is much shorter than the other two. All reactors have 10 cm distance between the lights.*

### 3.3.2 Reactor outlet

It was thought that some of the cyclones had problems with gas bypassing the reactor without swirling in the desired circular motion. It was thus decided to try if a different outlet would have an effect on the conversion. This was done by adding a so called *outlet tube* made out of quartz on the inside of the outer light sources. It was thought that this would avoid bypassing, with the air first flowing on the outside of the outer lamps and then, after changing direction at the bottom of the reactor, going on the inside. The use of quartz was to allow propagation of UV light through the tube.

These reactors with a different outlet were compared to the earlier tried geometries. They are shown below in Figure 10. All of the reactors have outlet tubes of 20 cm length, except case F2, which has a 13 cm long tube, to just cover the area where the inlet is situated.

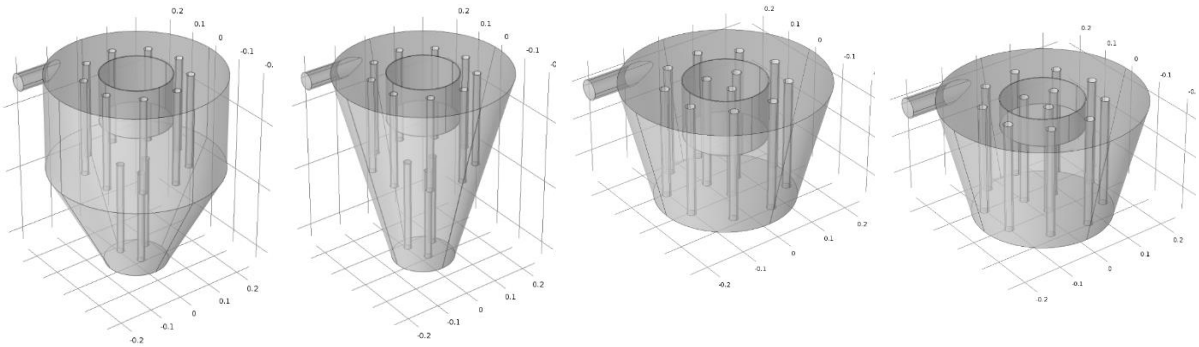

*Figure 10. The reactors tested with a different outlet, using a quartz tube to direct the fluid flow to not go directly from the inlet to the outlet. From the left; case D, E, F1 and F2.*

### 3.3.3 Lamp distance

As the cyclone geometry does not have the flow going straight perpendicular to the lamps it was thought that the lamp distance may differ in these reactors compared to the cubical reactors. Thus different

distances between the lamps was also evaluated with this geometry. In this configuration the cyclone reactor has lamps both in the upper and lower part of the reactor. Thus this lamp placement is very different from the cubical reactor. There are many different distances between the lights to consider, this is described below and shown in Figure 11.

- Distance between the center of the reactor and the inner lights (placed in the lower part of the reactor), shown in red. Called *a*.
- Distance between the inner lights and the outer lights (placed in the upper part of the reactor), shown in blue. Called *b*.
- Distance between two outer lights, shown in green. Called *c*.
- Radius of the reactor, shown in yellow. Called *r*.

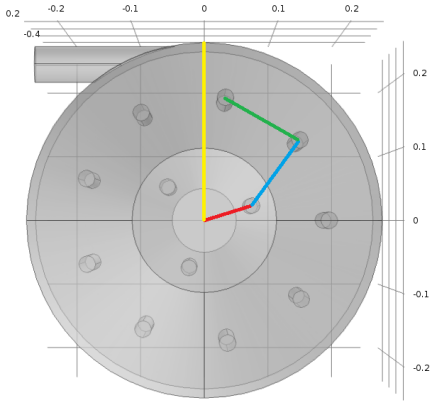


*Figure 11. The distances in the cyclone reactor.*

The different distances for the six reactors in the lamp distance test are written in Table 2 below.

*Table 2. The case numbers and all the distances between the lights together with the radius of the reactor. The cases marked with * are mainly used for the earlier trials and only here for comparison.*

| Case | Distance [cm] | | | |
|---|---|---|---|---|
| | a | b | c | r |
| A1* | 4.3 | 10.0 | 10.0 | 12.3 |
| G | 7.3 | 10.0 | 18.1 | 12.3 |
| H | 15.9 | 10.0 | 18.1 | 20.7 |
| I | 7.3 | 10.0 | 12.1 | 12.3 |
| J | 1.5 | 10.0 | 8.0 | 12.3 |
| C* | 4.3 | 10.0 | 10.0 | 12.3 |
| K | 9.0 | 5.3 | 10.0 | 12.3 |
| L | 4.3 | 4.3 | 6.0 | 12.3 |
| M | 1.5 | 3.0 | 3.1 | 12.3 |

In Figure 12, the geometry of the reactors with the distances in Table 12 are shown. The reactors are here shown as a cross-section of the xy-axis, looking through the whole reactor with all light sources showing.

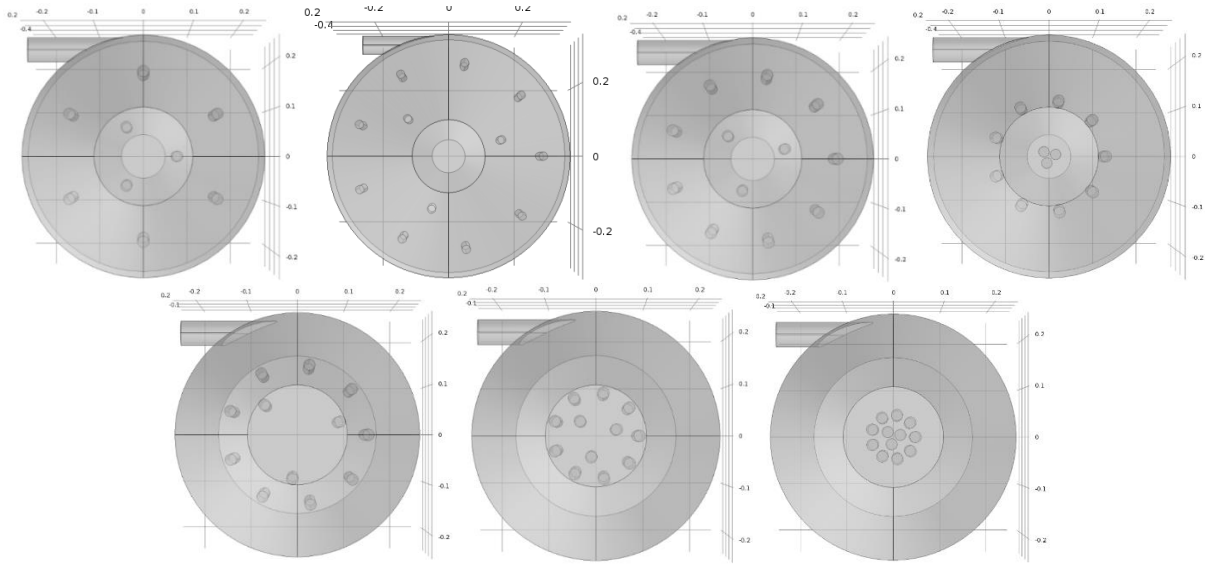

*Figure 12. The six reactors in the lamp distance trial for the complex geometry. Showing the distance between the lights. Top left; G, H, I and J. Bottom left; K, L and M.*

# 4. Results and Discussion

The results are divided into different sections; First, one section describing the results from the cubical reactors and then one section describing the more complex cyclone reactors. Finally, the results are summarized and discussed.

As mentioned above, several simplifying assumptions were done to facilitate time efficient simulations, thus the results obtained in this work will not give the exact answer to how well the reactors will perform in field. When comparing many different reactors as in this project, assuming that the simulation takes the most important factors of the reactor and its reactions into account, also assuming that the simulation does this in a good enough approach. Then it is possible to say that one reactor is going to perform with a higher conversion than the other. However, the results are to be seen as indications, not absolute values. Only a real field trial will answer exactly how well the reactors will perform.

## 4.1 Simulation – cubical reactor

A summation of all conversions given by the different simulations of the cubical reactors are shown in Table 8 in the *Appendix*.

### 4.1.1 Reference reactor

Case 1 represents the reactor used by Centriair today, scaled down into a prototype scale. This reactor has, according to the simulation, a conversion of 20.9 % when no after treatment is used. Zhang et al. [60] showed that the reactivity of aldehydes is proportional to the length of the carbon chain, thus acetaldehyde can be regared as comparably stable. Therefore, the conversion of this compound does not reach the ones obtained in the reactors in use today. However, as the conversion is far from complete conversion, it is easy to notice differences in the results when making changes to the reactor, which is desired in this project.

This reference was also simulated using amalgam lights (case 2), which has a three times higher current, the simulation was also given a three times higher flowrate, to have an equivalent current/flowrate ratio. The efficiency was assumed equal for both of the light sources, giving a conversion of 21.4 % for the amalgam lamp, which means that a higher Reynolds number would not influence the conversion significantly.

### 4.1.1.1 Reference geometry

The reference reactor has two rows of lamps straight after each other, as seen in Figure 14, where a cut at the zy-plane of the reactor is showing both the geometry in this angle (left) and the VOC outlet concentration (right).

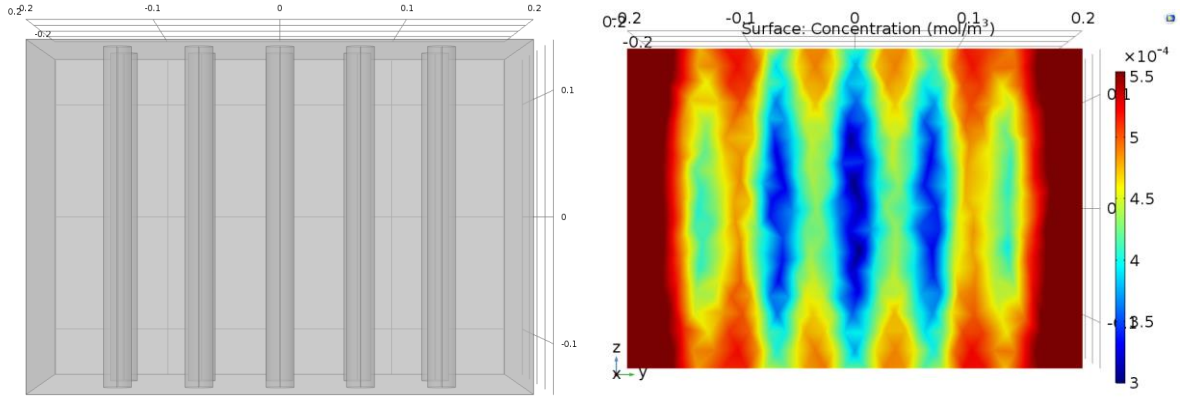


*Figure 13. Showing the zy-plane at the outlet of the reference reactor. Reactor geometry to the left and VOC outlet concentration to the right. The colors of the VOC outlet concentrations show concentration gradients; where blue is low concentrations ($3x10^{-4}$ mol/m$^3$) and dark red is high concentrations ($5.5x10^{-4}$ mol/m$^3$).*

When placing lamps in a row, some of the flow, often in the middle of the reactor, will be highly effected by the radiation which leads to a low concentration of VOCs (shown in blue). While other parts of the gas instead will flow beside the walls and is then only slightly affected by the radiation, which means that these flows will have high concentration of VOCs (shown in red). Thus, there will be very different concentrations of VOCs in different parts of the outlet. It is seen clearly in the right part of Figure 14 that this type of reactor creates bypassing; both against the wall of the reactor and in between the lights. It is especially clear against the wall, where the high concentration of VOCs is shown as dark red sides in the right part of Figure 14.

If this reference reactor was optimized using the same geometry, the bypassing effect would still remain. Thus, this type of reactor would never reach an efficient full VOC abatement potential. When not using mixers it is the geometry which will decide how the flow moves and if dark zones exist or not. Therefore, it was concluded that the geometry of the reactor is very important. As it will be the basis, central to if the reactor can reach an efficient full potential or not. Therefore, geometry research is crucial for optimizing the performance of a UV reactor.

## 4.1.2 Lamp distance

The lamp distance simulations were carried out with the lamps in a hexagonal pattern. This configuration allowed all the lamps to have the same distance R from each other. When looking at the conversion results for the lamp distance trials, the green bars in Figure 13, there is a clear correlation between the increase of lamp distance and the conversion.

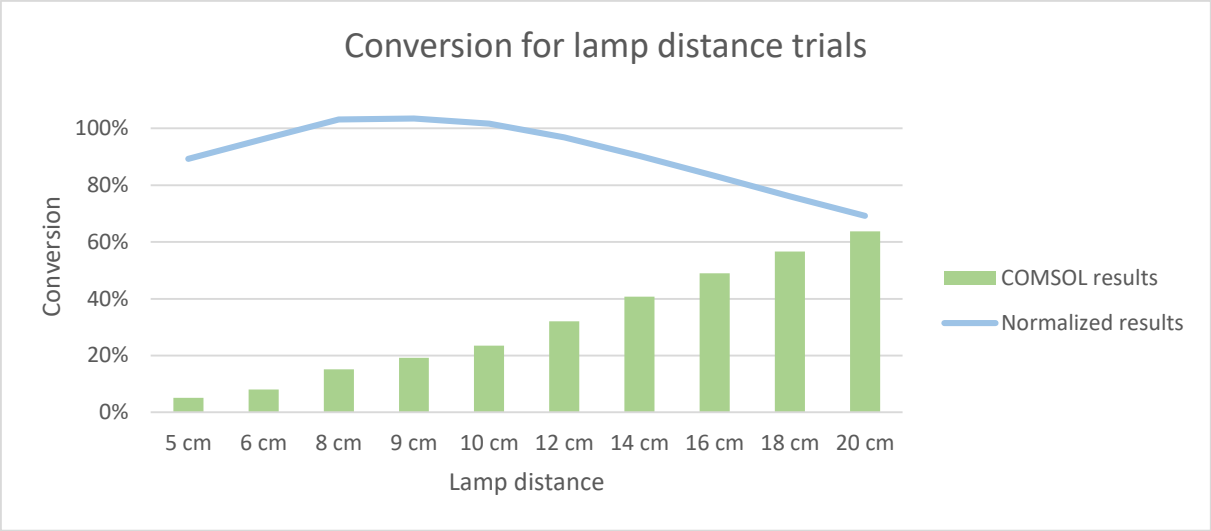


*Figure 14. The conversion for the ten cases of lamp distance simulations. The blue line shows the normalized results, where the conversion can be compared independent of the volume of the reactor and number of light sources. The normalized results are also in relation to the reference reactor, which represents 100%.*

These green bars represent the conversion obtained from the COMSOL® simulations. The increase of lamp distance will, as stated in the Method, also mean that there is an increase in reactor size. Even though the reactor size will have an influence on the conversion due to increased residence time, the linearity of the conversion results together with the earlier described limitations of the irradiation model found by Jacob and Dranoff [53], suggested the idea of normalizing the results. The normalization made it possible to compare reactors of different sizes and with different number of light sources. The results were normalized by dividing the conversion result with the reactor volume and the number of lamps. This was then divided with the normalized result from the reference reactor, to keep all the results in relation to this reactor, which represents 100%. Therefore, if a reactor has a conversion result of 88% it has a 12% lower conversion than the reference reactor, while a conversion of 115% is 15% better. In Table 8 and 9, in the *Appendix* both the results obtained from the COMSOL® simulations and the normalized results are shown. However, in the rest of this Results and Discussion section only the normalized results will be discussed for all simulations and can be referred to either *normalized conversion* or just *conversion*.

When looking at the normalized results (blue line) in Figure 13 it is clear that there is an optimum distance between the lamps. This is at the span of 8-10 cm distance, as 9 cm has a normalized conversion of 103.4% and both 8 and 10 cm are close thereafter with conversions of 103.1% respective 101.7%. At shorter distances there is too little time for the degradation to happen, if more lights with this distance were placed in a larger reactor the conversion would presumably increase. However, as the light source is the energy consuming part of the reactor, more light sources than necessary is not desired. At longer distances, the irradiation will not reach all the gas, thus creating dark zones and irradiation bypassing.

The distance of 8-10 cm is the optimal compromise between residence time and gas irradiation.

### 4.1.4 Lamp geometry

Seven different lamp geometries were simulated to see what effect the lamp placement had on the conversion. In Table 3 there is a short description of these cases.

*Table 3. A summary of the reactors used in the lamp geometry trials.*

| LAMP GEOMETRY CASES | |
|---|---|
| **Case** | **Description** |
| **3** | 2 rows, staggered lamps |
| **4e** | Hexagonal, R=10 cm |
| **5** | Horizontal and vertical lamps |
| **6** | Two lamps in five rows |
| **7** | 3 amalgam lamps |
| **8** | Hexagonal, flow along y-axis |
| **9** | Hexagonal, flow along z-axis |

Figure 15 shows the normalized conversion obtained for the different cases, it is clear that there is only one case which performed better than the reference reactor in terms of conversion, case 4e, which is the reactor with lamps in a hexagonal configuration (10 cm distance) as in the lamp distance test.

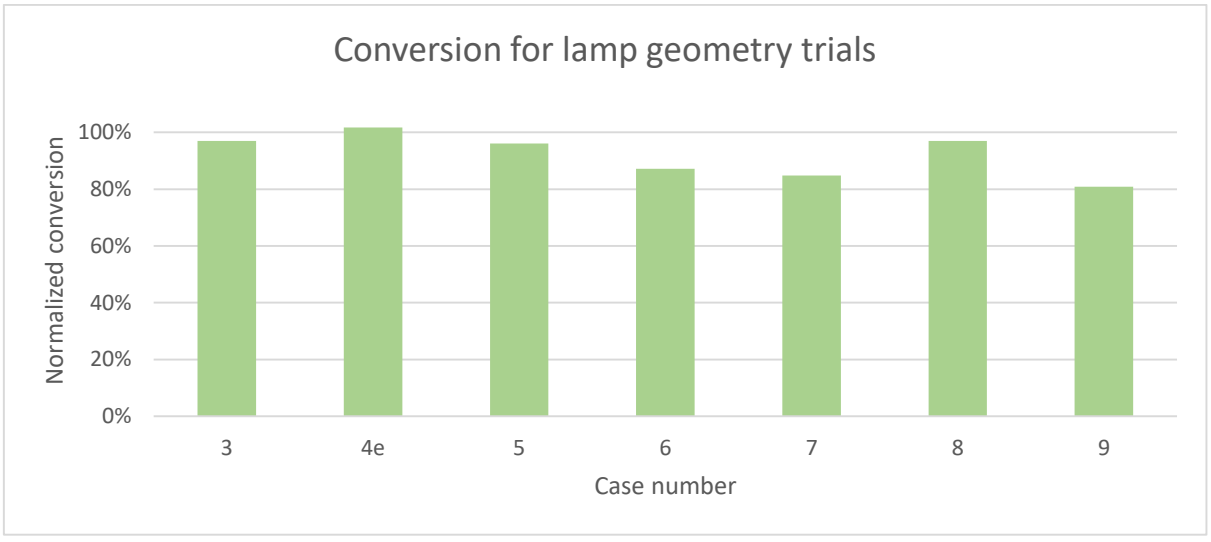


*Figure 15. The normalized conversion results from the lamp geometry trials.*

Case 4e outperformed the others due to a very close to optimal distance between the lights, while minimizing bypass. Case 9 which has the lowest conversion is the only reactor where the gas flow goes along the length of the lights, i.e. along the z-axis. As the result is so low, this does not seem to be an optimal geometry for VOC degradation. Also, looking at a cut of the xy-plane showing the VOC outlet concentration, in Figure 16, where most of the figure is red, indicating high concentrations of VOCs.

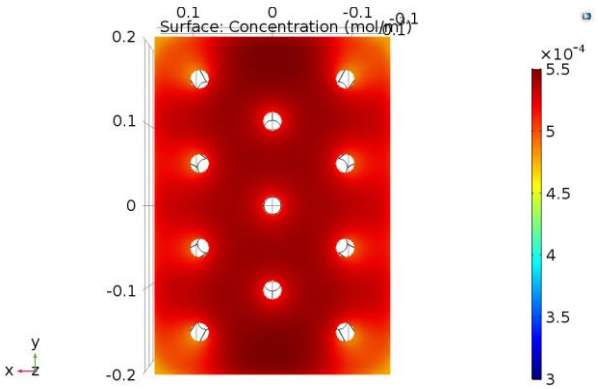


*Figure 16. The VOC outlet concentration of case 9 which is has a hexagonal lamp configuration with a flow along the z-axis.*

It is thus clear that this lamp placement together with the flow direction causes the flow to just pass the lights without being greatly affected by the irradiation. This could be due to the gas flow not hitting the lights, as it does when the flow is perpendicular to the lamps. Thus, the speed of the gas flow will not decrease, which means that the gas will have a shorter time by the light. However, it is possible that this would be a better configuration if the lights were positioned closer to each other or if the flow was directed closer to the light source with a static mixer, as shown by Wols et al. [9].

Both case 6 and 8 have gas flowing along the y-axis, case 6 with five rows of lamps straight after each other, while case 8 has a hexagonal lamp configuration. This means that they will pass several more rows of lights even though they pass the same amount of light sources as in the corresponding configurations with the flow along the x-axis; Case 1 and 4e. It was believed that the VOCs would have a longer time to react when doing so, thus the conversion might be higher. However, as these reactors both have lower conversions than the reference reactor, as seen in the diagram in Figure 15, this was not the case. Case 6 had a serious case of bypassing as shown in Figure 17 where a cut of the xz-plane is showing the VOC outlet concentration. This figure has mainly dark red parts, which is parts with high concentration of VOCs.

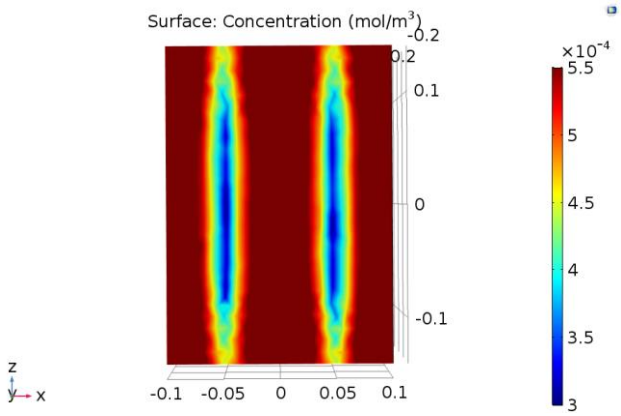


*Figure 17. The VOC outlet concentration in the xz-plane for case 6.*

The hexagonal pattern in case 8 reduced the bypass, but this case still had more bypassing than in case 4e when the gas flowed along the x-axis. This comparison is seen in Figure 18 below where the outlet concentration of VOCs is shown, the reactor to the left has a flow along the x-axis, case 4e, and the right a flow along the y-axis, case 8.

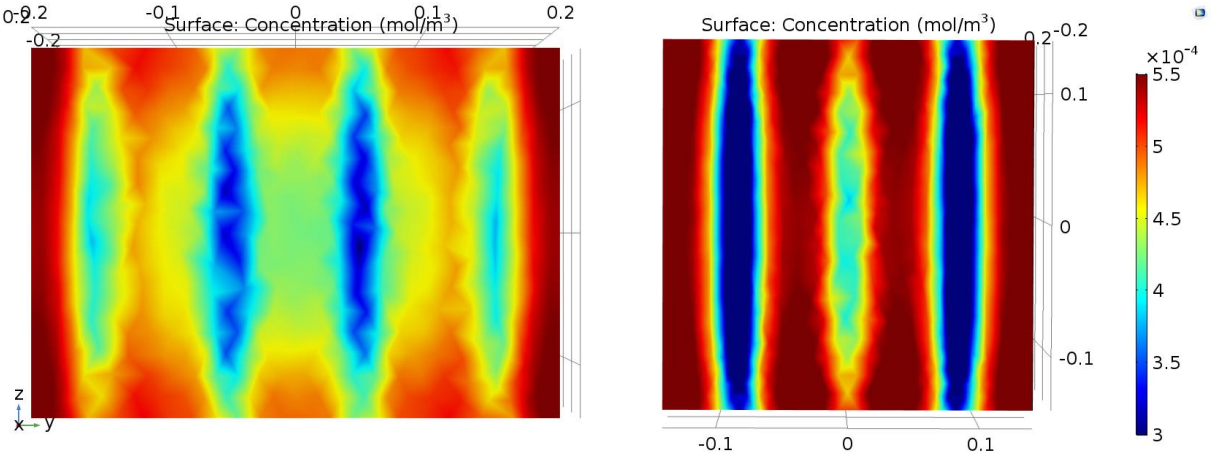


*Figure 18. VOC outlet concentration for case 4e (left) and case 8 (right). Both have hexagonal lamp configuration, however case 4e has a flow along the x-axis, while case 8 has a flow along the y-axis.*

It is clear that the colors lean more towards green and blue in the figure to the left, indicating lower VOC concentrations. In the right figure there are four clear bands colored dark red, which indicates the bypassing problem in this reactor. In the left figure there is mainly heavy bypassing by the wall of the reactor which is shown as thin dark red bands on the sides of the figure.

The results show that placing the lamps in a pattern which does not form straight rows lead to a higher conversion, as there will be less free space on especially the sides which will give less extreme cases of bypassing. As soon as there is space where the gas can flow straight without hitting a light source or some other solid object, the bypassing effect will appear which in turn will give a lower conversion.

Case 5 has both horizontal and vertical lamps, therefore it was believed that this would help solve some of the bypassing, especially by the walls. As the light sources only are 28 cm, but the reactor base is 40 x 40 cm it was decided to have the horizontal lamps placed every other sticking in from the left side of the reactor and the rest from the right side, creating a zigzag pattern.

This configuration did however, not perform as good as expected. It increases the mixing of the flow, which is seen in the VOC outlet concentration, to the right in Figure 19, where the colors in the center are more homogeneous.

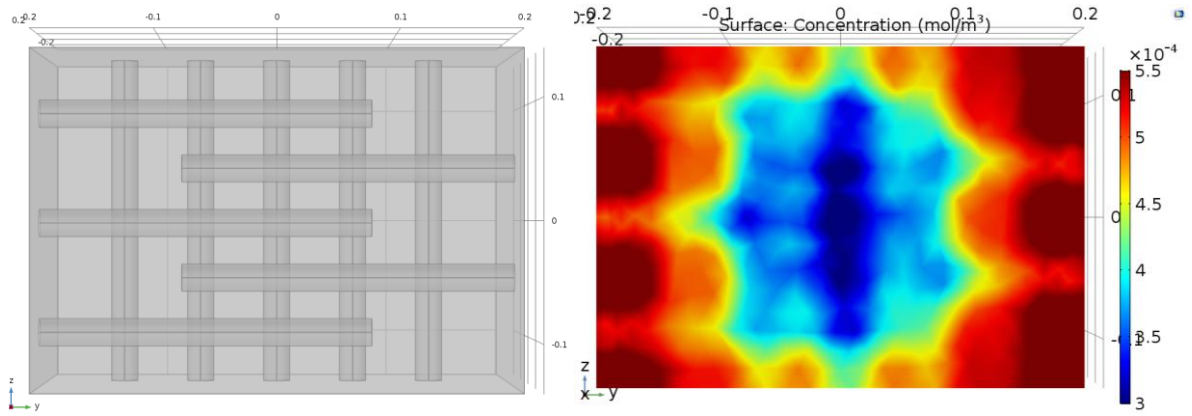


*Figure 19. The zy-plane at the outlet of case 5. Reactor geometry to the left and VOC outlet concentration to the right. This case has both horizontal and vertical lamps.*

Yet, it still had a large bypass against the walls of the reactor. This is due to the horizontal lamps together with the vertical lamps contribute to emitting more irradiation at the center. While the sides only had horizontal lights. Furthermore, as the horizontal lights were added in a zigzag pattern there were three lamps on one side and two on the other, as seen in the geometry to the left in Figure 19. It is also seen to the right in Figure 19, where there are three light red lines on the right side and only two on the left. This configuration would increase the conversion if it could be built in four rows; two horizontal and two vertical. Nevertheless, the hexagonal pattern would still have a higher conversion according to these simulations.

Another way of minimizing the bypassing might be to use case 3, where the two rows of lamps are staggered. Staggering means that the lamps are not placed straight after each other, instead they form a zigzag pattern. In this case only vertical light sources were used. This means that there would be one lamp in each row which is closer to the wall on each side. Yet, this did not perform better than the reference reactor. This, as many of the above described reactors, also had a bypassing problem at the walls as shown in Figure 20.

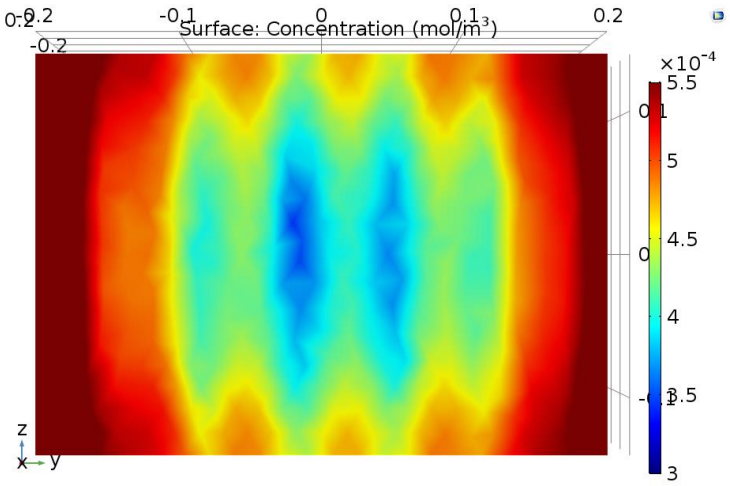


*Figure 20. The VOC outlet concentration of case 3, with staggered lamps forming a zigzag pattern using only vertical light sources.*

It is due to the fact that there is only one light close to the wall, which is not enough to take care of all the VOCs in this region. If a solid object would be used to force the flow closer to another light after or before this one light, the conversion would presumably be higher.

Further, it may be observed that the bypass is slightly more severe on the left side of the reactor outlet. This is due to the single lamp by the wall is in the last row of lamps on this side. Therefore, there is less time to degrade the VOCs compared to the right side where the single light is in the first row of lamps.

Case 7 was simulated to see if there really is a need for a high number of low pressure lamps, or if it is possible to have just three amalgam lights instead. As amalgam light have three times higher current, this would correspond to the power of nine low pressure lamps. Using a smaller number of light sources will mean a lower investment cost and less maintenance as there are less lamps to maintain. However, as the conversion of this configuration was much lower than the reference reactor, this seem to not be a feasible alternative in UV reactors used for VOC degradation. The reason being the dark zones that seems to be occurring when there is a large distance between the lamps. The price vs. conversion compromise will have to be discussed from case to case, but as the aim of this thesis is to reach a higher conversion it will not be further discussed here.

### 4.1.5 Fluid dynamics

As shown above there is an important limitation with dark zones and thus bypassing in the UV reactors. As stated in the Literature Review this can be solved by introducing more turbulence or by forcing the gas to flow closer to the light sources. This was the aim of the fluid dynamics trials. In Table 4 below a short description of all the cases is shown.

*Table 4. A summary of the reactors used in the fluid dynamics trials.*

| FLUID DYNAMIC CASES | | |
|---|---|---|
| **Case** | **Description** | **Vortex generators [nr x rows]** |
| **10a** | 2 straight rows lamps | 3x1 |
| **10b** | 2 straight rows lamps | 3x2 |
| **11a** | Hexagonal, R=10 cm | 3x2 |
| **11b** | Hexagonal, R=10 cm | 3x3 |
| **11c** | Hexagonal, R=10 cm | 9x3 |

In Figure 21 below the normalized conversion results are shown for the turbulence tests.

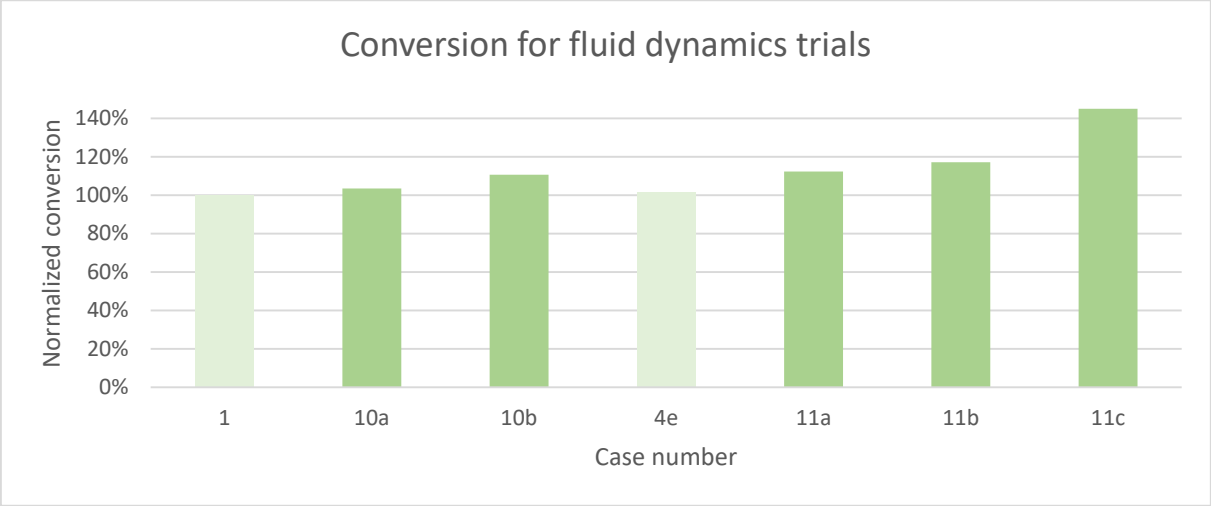


*Figure 21. The normalized conversion for the cases with vortex generators inside the reactors.*

As in the lamp geometry simulations, the reactors with lamps placed in a hexagonal pattern, case 11, has a higher conversion than the ones with two rows of lamp straight after each other, case 10. These are compared to the light green bars, which are reactors with the same lamp geometry and size, but without vortex generators. Case 1 has its lights straight after each other and 4e has a hexagonal pattern. Both case 10 and 11 are have higher conversions than case 1 respective 4e.

From these results it is also clear that the cases named b show higher conversion than the ones named a, the only difference between these cases is that both case 10b and 11b have one more row of vortex generators than case 10a and 11a. It is also noted that case 11c has a much higher conversion than the other ones. This case has more vortex generators in three rows; nine small ones compared to three larger ones which constitute case 11b.

The results in show that the vortex generators greatly improve the conversion in the UV reactors. Also, according to these results more vortex generators will give a higher conversion. However, in the simulations it is also possible to see that there will be a pressure drop when adding the vortex generators. This can be seen in Figure 22 below, where the pressure drops for case 11a and 11c are shown.

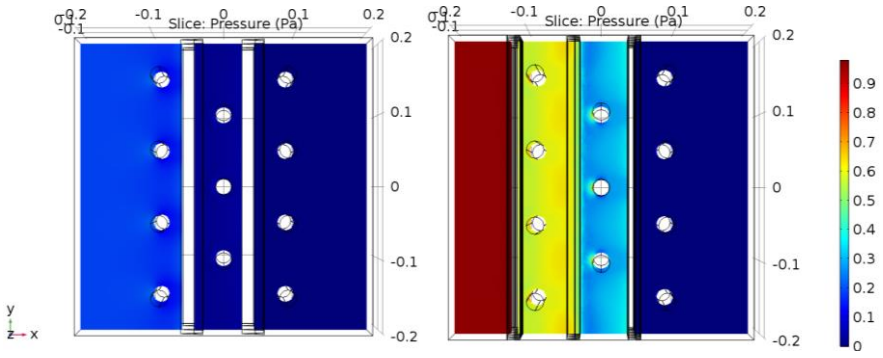


*Figure 22. The pressure differences inside case 11a (left) and 11c (right), given in $10^5$ Pa.*

It is clear that there is a much higher pressure drop in case 11c, as this starts at a higher pressure (red color) but still gets the same pressure in the end (dark blue color). As a high pressure drop is not desired, it is important to also look at this factor when designing a UV reactor with vortex generators. As long as the fluid can get past the generators without too high pressure drop it will be beneficial and give the reactor a higher conversion.

## 4.2 Simulation - Complex geometry

As the aim is to get a reactor with a higher conversion than the reference reactor, case 1, these complex geometries are thus also compared, normalized in relation to the reference reactor. Consequently, the reference reactor still represents 100% conversion, as in the results below. A summation of all conversions given by the different simulations with the complex geometry are shown in Table 9 in the *Appendix*.

### 4.2.1 Reactor geometry

Two main types of geometries were tested. One of traditional cyclone shape, case A, and another smoother more conical one, case B. Also, a short version of the smoother cyclone was simulated, case C. A short description of each case can be seen in Table 5 below.

*Table 5. A summary of the cases used for the reactor geometry trials.*

| REACTOR GEOMETRY CASES | | | |
|---|---|---|---|
| **Case** | **Description** | **b-distance [cm]** | **c-distance [cm]** |
| **A1** | Traditional cyclone | 10.0 | 10.0 |
| **A2** | Traditional cyclone, wider | 10.0 | 10.0 |
| **B1** | Smoother cyclone | 10.0 | 10.0 |
| **B2** | Smoother cyclone, wider | 10.0 | 10.0 |
| **C** | Smoother cyclone, short | 10.0 | 10.0 |

As seen in Figure 23 below, both case A1 and B1 showed a higher normalized conversion than the reference reactor. However, case B1 was slightly better with a conversion of 106.0% compared to A1 with 104.1%.

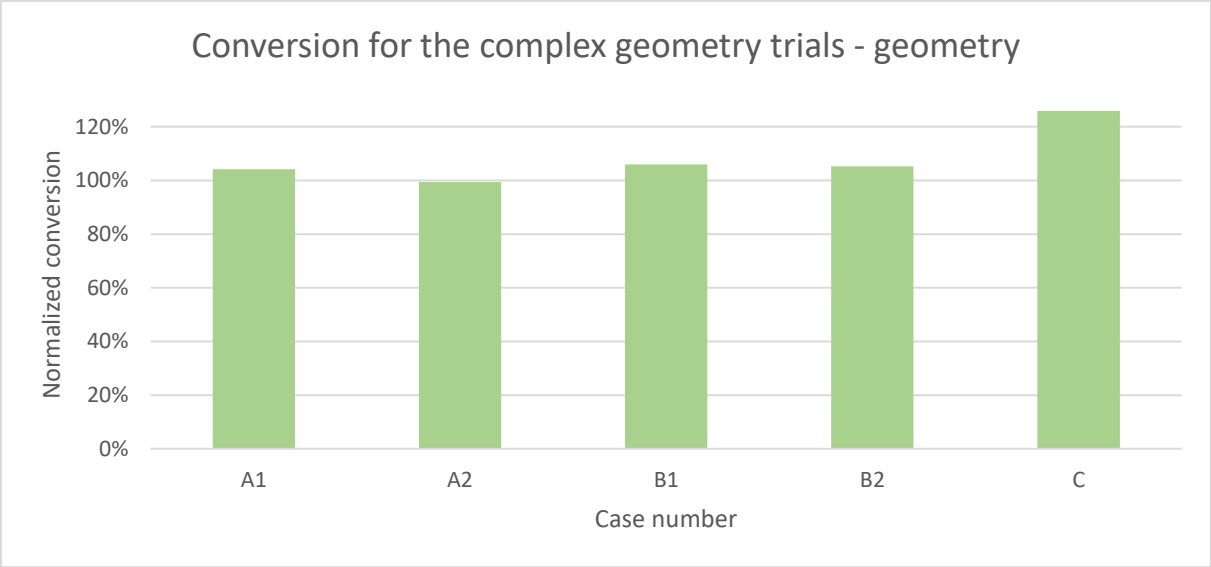


*Figure 23. The normalized conversion for the different cyclone reactor simulations.*

When looking at the fluid stream of the reactors, it seems like there was a large section at the bottom of the reactors which is not utilized. It was thought that the lamps were hindering the fluid from reaching the bottom. Thus, the reactors in case A1 and B1 were then made a little wider at the bottom. However, as shown in Figure 24 the widening of the reactors seems to have made the fluid flow worse. The conversion got lower and the fluid stream plot showed that the bottom of the reactor still was not fully utilized, showing the fluid stream plot for case B1 and B2. Case A had the same type of problem.

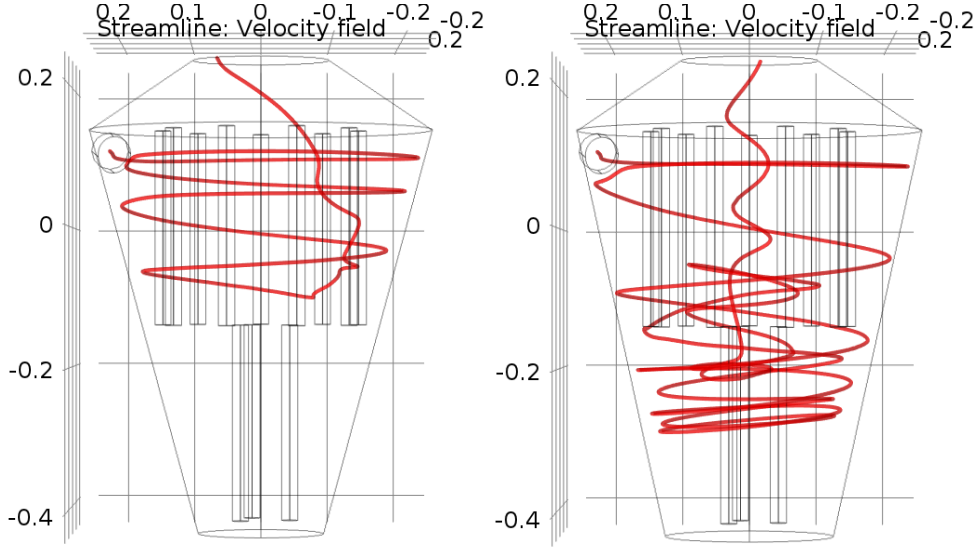


*Figure 24. Fluid flow pattern for case B1 (left) and B2 (right). The red line shows how the fluid flow is moving in the reactor.*

To solve the problem of not utilizing the whole reactor, case C was deviced. This is case B1 cut in half, moving up all the inner light sources. As seen in Figure 25, the fluid will flow in the whole reactor, not forming any stagnant zones. Also, as shown in Figure 23, the conversion for this case is much higher than for case B1 and B2.

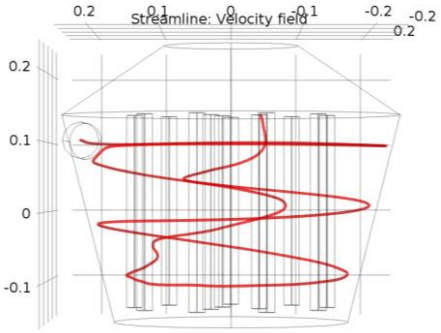


*Figure 25. The fluid flow in case C.*

### 4.2.2 Reactor outlet

The placement of the inlet and outlet may cause a risk of getting a traditional bypass, where the fluid will flow into to the reactor from the inlet and then go straight to the outlet without passing the lights in the wanted circular motion. Thus, a quartz outlet tube was placed in the outlet. In Table 6 below a short description of the cases is shown.

*Table 6. Summary of the cases used in the Reactor outlet trials.*

| REACTOR OUTLET CASES | | | | |
|---|---|---|---|---|
| **Case** | **Description** | **Outlet tube [cm]** | **b-distance [cm]** | **c-distance [cm]** |
| **D** | Traditional cyclone | 20.0 | 10.0 | 10.0 |
| **E** | Smooth cyclone | 20.0 | 10.0 | 10.0 |
| **F1** | Smooth cyclone, short | 20.0 | 10.0 | 10.0 |
| **F2** | Smooth cyclone, short | 13.0 | 10.0 | 10.0 |

Figure 26 shows the normalized conversions for the reactors with the added outlet tube together with some reactors without outlet tube for comparsion.

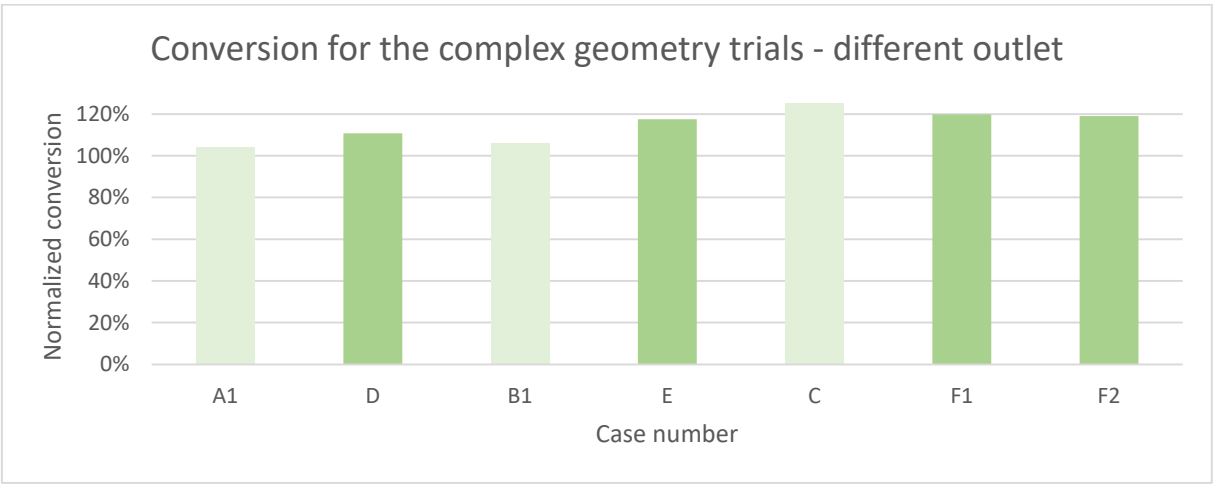


*Figure 26. The normalized conversion results for the reactors fitted with an outlet tube. The light green bars are reactors without outlet tubes, for comparison.*

From Figure 26 it is clear that for the larger cyclone reactors it is beneficial to have an outlet tube. Both case D and E show a higher conversion than case A1 and B1, which are the same type of reactor without the quartz outlet tube. However, for the shorter version of the reactor it seems to be unfavorable, as both F1 and F2 show a lower conversion than case C. This is due to the fact that the 20 cm outlet tube takes up half the reactor in the short cyclone. Also, to be able to fit all the light sources in the reactor, the inner lights have to be fitted inside the tube. This makes it very difficult for the gas flow to find its way out of the reactor. A shorter tube was also simulated, case F2, but still the conversion was quite low. This is likely due to that the inner lights are inside the tube, taking up space and making it harder for the fluid to reach the outlet.

### 4.2.3 Lamp distance

As the fluid in the cyclone reactor flows in a very different pattern than in the cubical reactor it was concluded that the effect of the lamp distance has to be evaluated for this configuration as well. A short description of each of the cases used in this trial is shown in Table 7 below.

*Table 7. Summary of the cases used in the lamp distance trial for the complex geometry.*

| COMPLEX LAMP DISTANCE CASES | | | | | |
|---|---|---|---|---|---|
| **Case** | **Description** | **a-distance [cm]** | **b-distance [cm]** | **c-distance [cm]** | **Lamps** |
| **G** | Traditional cyclone | 7.3 | 10.0 | 18.1 | 9 |
| **H** | Traditional cyclone, large | 15.9 | 10.0 | 18.1 | 12 |
| **I** | Traditional cyclone | 7.3 | 10.0 | 12.1 | 12 |
| **J** | Traditional cyclone | 1.5 | 10.0 | 8.0 | 12 |
| **K** | Smooth cyclone, short, inner lamps moved towards outer | 9.0 | 5.3 | 10.0 | 12 |
| **L** | Smooth cyclone, short, outer lamps moved towards inner | 4.3 | 4.3 | 6.0 | 12 |
| **M** | Smooth cyclone, short | 1.5 | 3.0 | 3.1 | 12 |

In Figure 27 it is seen that the closer the outer lamp is to the center of the reactor the higher the conversion.

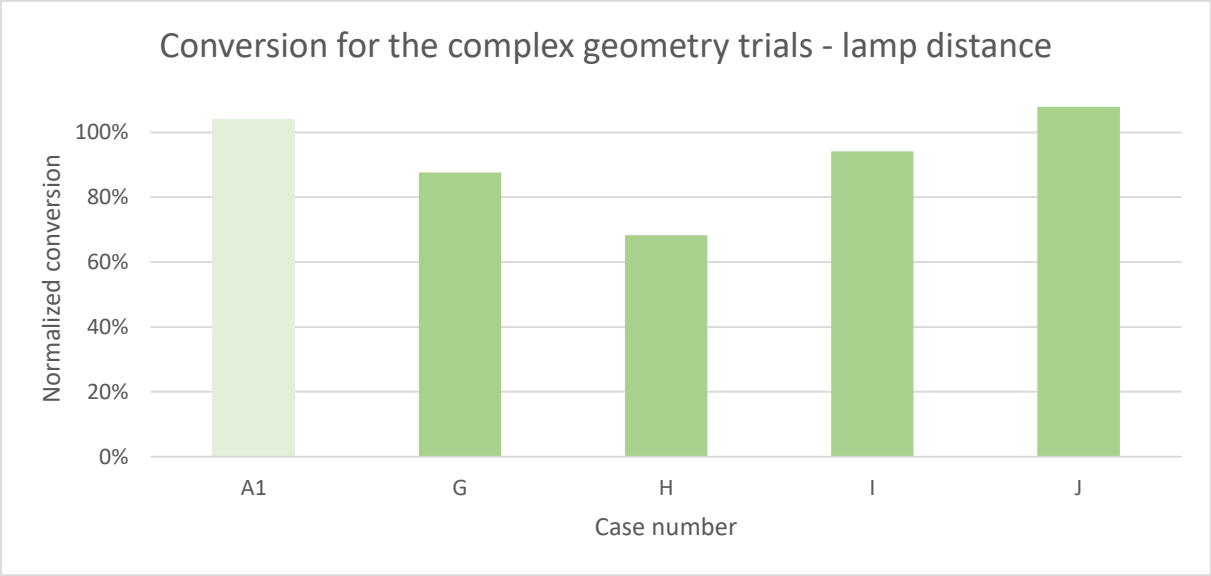


*Figure 27. The normalized conversion results from the lamp distance trials on the cyclone geometry. The light green bar is a reactor with 10 cm in both distance b and c, for comparison.*

The bar in light green in the diagram is the comparison case, case A1, which has both distance b and c set to 10 cm. The largest reactor, case H, has the lowest conversion. Just like in the lamp distance optimization for the cubical reactor, this is due to a too large distance between the lights. The low conversion in this case can be explained by dark zones where the irradiation will not reach all of the gas.

The second to lowest was case G, in this case distance b and c were as large as in case H, but distance a was shorter. The gas then managed to get more irradiation and consequently a higher conversion was obtained.

Also case I showed a lower conversion than the comparison reactor. Case I had the distance c set to 12 cm, with distance b maintained at 10 cm. Case J had a shorter c distance than A1, set to 8 cm, still keeping the b distance the same. A short c distance will mean a shorter perimeter which in turn will mean a shorter distance between the outer lamps and the center of the reactor. As the conversion gets higher with the shorter c distance it can be concluded that the closer the lamps are to the center of the reactor, the better.

Consequently, in the short reactor test with case C, K, L and M shown in Figure 28, the effect of the distance between the outer and inner lights, distance b, was simulated.

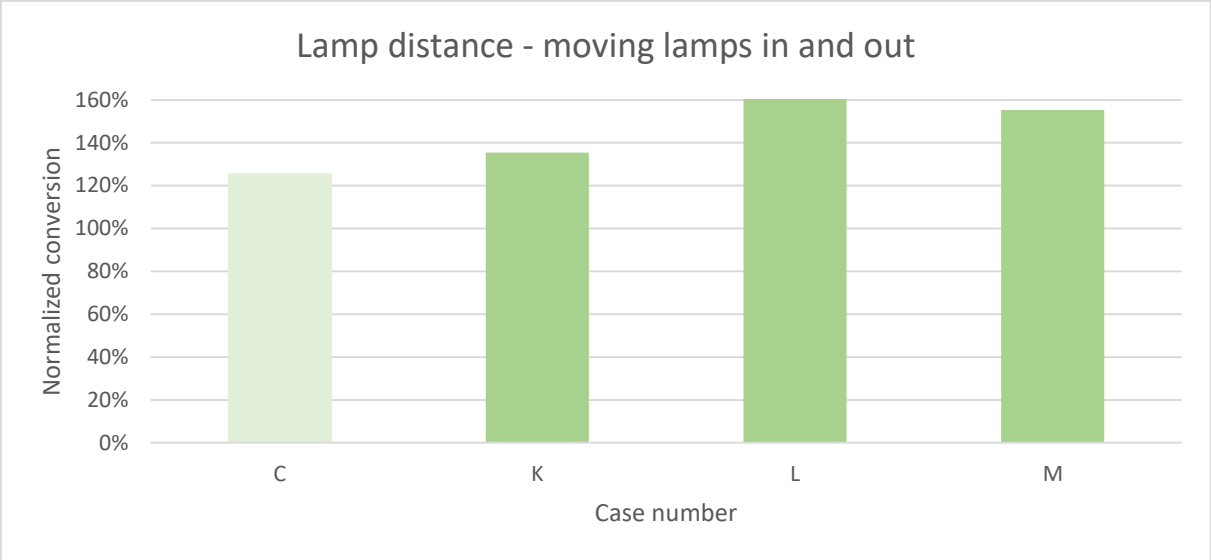


*Figure 28. The normalized conversion from the lamp distance simulations on the short reactors, where the inner lamps were moved towards the outer in case K, the outer lamps were moved toward the inner in case L and everything was moved to the center in case M. The light green bar is a reactor with 10 cm in both distance b and c, for comparison.*

Here the comparison case, case C (light green bar), which has the a distance set to 4.3 cm and the b and c distances set to 10 cm, is the one with the lowest conversion. Case K has the inner lamps moved closer to the outer ones, while case L has the outer lamps moved in close to the inner lamps and case M has everything moved to the center of the reactor, i.e. case K has the same c distance as case C, but a longer a distance. While case L has the same a distance as case C and both the b and c distances are shorter. Both these, especially case L, has a much higher conversion than the comparison case C. Case M instead has all the distances set as short as possible.

When looking at case K and L it can be concluded that it is better to move all the lamps closer to the center of the reactor due to the fact that the gas will be able to rotate several more times around the lamps before it moves into the center and towards the outlet. This can be seen in Figure 29, where a comparison is made between the fluid flow in case C (left) and case L (right).

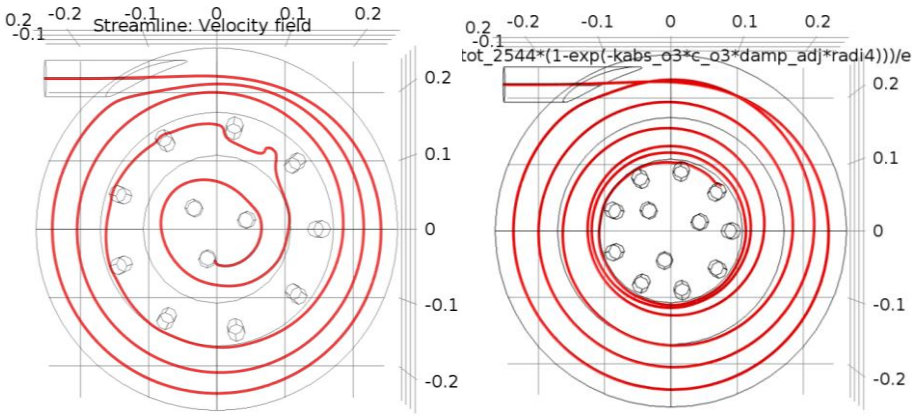


*Figure 29. The fluid flow in case C (left) and L (right). It is here seen that the fluid will rotate several more times in the reactor before it leaves case L compared to C.*

As the lamps are closer to each other in case L, they have a lot more ozone decomposition in the center, which means a higher conversion of VOCs in this area. This is due to the narrower distance between the lamps, which will lower the velocity in the center. As stated in the Literature Review, it is important that the polluted gas not only is irradiated in a homogenized manner. It is also important that the gas gets enough time by the light source, such that the ozone will have time to form. The outer part of the reactor in case L will handle mixing while also irradiating the gas. While the inner part will mainly produce and thus also decompose ozone, such that when the VOC reaches this area it will be decomposed by these radicals formed by the ozone. This can be seen in Figure 30 below, where a comparison of the ozone decomposition in case C (left) and case L (right) is shown.

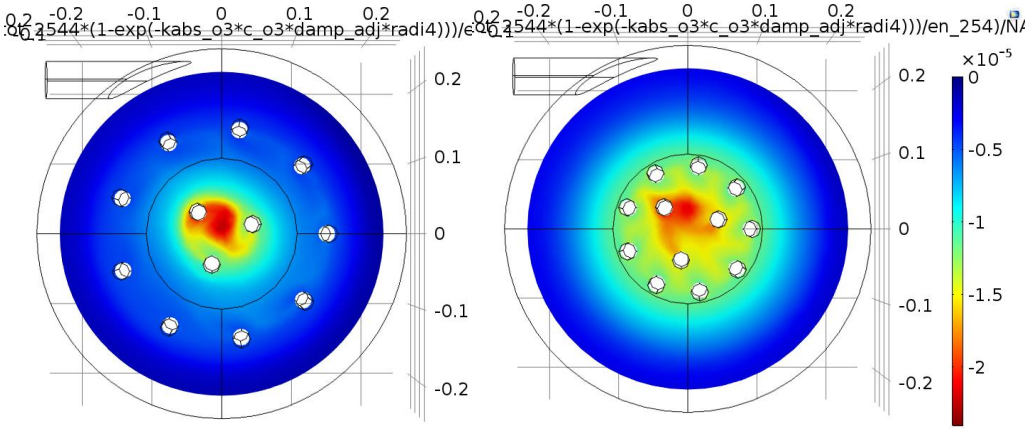


*Figure 30. The ozone decomposition rate of case C and L. A blue color indicates a low decomposition rate and the red color shows a high decomposition rate. It is clear that the decomposition rate for case L is higher.*

The blue color represents a low decomposition rate and the red color means a high decomposition rate. It is clear that there is a much larger area with high decomposition rate in case L, thus the VOC decomposition will also be higher in this reactor.

When looking at both Figure 29 and 30, it is seen that the flow stream of the fluid in case L circles the outer part of the outer lamps several times before flowing into the outlet. This is also one of the parts where, according to Figure 30 the ozone decomposition is higher, thus also the VOC decomposition. Therefore, case L creates a higly favorable environment for VOC decomposition.

It can be concluded that for a cyclone reactor it is better that the inner and outer light sources are placed close together. This is due to the fact that the circular flow in a cyclone will be interrupted when encountering an obstacle. If all the lamps are placed close to the center and also close together, the flow will be able to circulate without getting interrupted. Also, a flow which is not interrupted will rotate a larger number of times before exiting the reactor, leading to a longer residence time, and thus a higher conversion, just like both Jeong et al. [10] and Chang et al. [11] showed in their research.

As it was concluded that the lamps should be as close to the center as possible, one more simulation was carried out, Case M. In this case the light sources were placed as close to the center of the cyclone as

possible. This case however showed a slightly lower conversion than the above described case L. When looking at Figure 31 below, it is clear why this is the case; The flow in this reactor has the same pattern as in case L, however, as the light sources are closer to the center the main flow will not be as close to the lights as in case L.

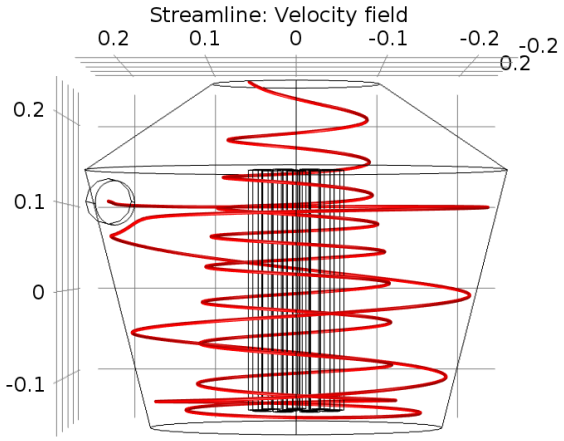


*Figure 31. The main stream flow for case M, where the lamps are situated as close to the center of the reactor as possible.*

The conclusion is then that the lamps should be situated as close to the center as possible, without getting too far from the main flow field. This distance will depend on the cyclone size, as the size determines what the main flow field looks like.

Another possible reason for why case M gets a lower conversion is that there is less space to produce ozone. As the area between the lights is smaller there will be less volume of air, therefore there is also less compounds to be converted into ozone. Less ozone means less VOC conversion.

## 4.3 Summary

Even if some limitations to the irradiation model were found, the normalization made it possible to compare the different reactors. The normalization made it easy to see that there was an optimum in the distance between the lamps in the cubical reactor. At 8-10 cm the conversion was highest, when using a hexagonal lamp configuration. When looking at the lamp configuration, it was also noted that the hexagonal configuration in fact was the best of the ones tried. The reason presumably being that this configuration showed the least dark zones.

Just like stated in the Literature Review, creating turbulence was one of the keys to obtaining a higher conversion. The more vortex generators the better, as long as the pressure drop is not too high. The vortex generators allowed the flow to stay a longer time close by the light sources, while also mixing the fluid. This is a good combination, giving the highest normalized conversion for the cubical reactors when using 9x3 vortex generators; 45% higher than the reference case.

When looking at the more complex geometry, the cyclone reactor, it was noted that a smooth conical reactor was preferred over a traditional cyclone reactor. After realizing that not the whole reactor was utilized it was cut in half, moving all of the lamps up to the same level. Just by changing the geometry of the reactor the conversion was already at a level of almost 126%.

Many cyclones have a so called outlet tube. This is to stop the fluid from moving straight from the inlet to the outlet, without first circulating in the reactor. This type of outlet was simulated, using a quartz outlet tube, to allow the irradiation to pass through. This was a promising configuration for the larger cyclone reactors with lamps in two levels. However, for the short version of the cyclone this was not an advantage, as it made it harder for the flow to exit the reactor.

The cyclone has such a different geometry than the cubical reactor, also the fluid flows in a very different way. Thus, it was decided to look at the lamp distance also in this geometry. In these trials a specific optimum was never found in the distance between the lights. However, it was concluded that the closer to the center of the reactor the light sources were placed, the better, as long as the lamps are not situated too far from the main fluid stream. However, it was also found that not to interrupt the fluid flow, the optimal was to have the inner and the outer lights close to each other. If these recommendations are followed normalized conversion 61% higher than the reference reactor may be reached according to the simulations. However, as the simulations were performed under a number of simplifying assumptions, the values obtained should not be seen as absolute values, instead as indications.

It was concluded that the biggest issue with a UV reactor up-scaling and optimization is the dark zones and the bypassing effect given by these. It is thus very important that the irradiation reaches the whole reactor and that all gas is affected by it. It is also important that the gas is given time to stay by the light sources as long as possible. The optimized cyclone reactor, case L, is a very promising candidate to overcome these problems.

# 5. CONCLUSIONS

The conclusion from this work is that the biggest issue with a UV reactor up-scaling and optimization is the dark zones and the bypassing effect given by these, just as many other researches stated previously [9], [10], [11]. As specified in the Literature Review, it is very important that the irradiation reaches the whole reactor and that all gas is affected. It is also important that the gas is given time to stay by the light sources as long as possible. As it is not possible to have a very low velocity or a very large reactor, this has to be managed with the reactor geometry and/or solid objects like vortex generators. These factors have to be considered at an early stage when designing a UV reactor.

A good way of dealing with these problems is by using a hexagonal lamp configuration with a distance of 8-10 cm between the lamps, also using vortex generators in between the rows of lamps. Also, a very promising UV reactor geometry is a short cyclone with the inner and outer light sources close to each other, situated close to the center of the reactor without being too far from the main fluid stream. As these were the reactors with the highest normalized conversion results in this project; 145% respectively 161% of conversion. This is a quite large improvement, when comparing to the reference reactor which is used today by Centriair, which is represented by 100% conversion in this project. With these results it is clear that changes are needed to today's geometry. The cyclone geometry is the most promising.

However, as with any simulations there are assumptions made which can affect the results. The simulation will not give the exact answer to how well the reactors will perform in field. When comparing many different reactors as in this thesis, assuming that the simulation takes the most important factors of the reactor and its reactions into account, also assuming that the simulation does this in a good enough approach. Then it is possible to say that one reactor is going to perform with a higher conversion than the other. However, the results are to be seen as indications, not absolute values. Only field trials will answer exactly how well the reactors will perform.

As George Box ones said: "*All models are wrong but some are useful*" [1].

# 6. FURTHER RESEARCH

As this project is still only at the simulation stage of the up-scaling process, there are several areas which could be further investigated, some are presented below.

- Experimental verification of the simulations, i.e. field trials.
    - Using the reactors suggested in this thesis. Mainly to confirm that the indications given in the simulations are correct.

If the indications of the simulations in this thesis are confirmed, the following areas should be looked into further.

- Solving the model's irradiation limitations.
- Adding additional reactor information to the model. Mainly the following points.
    - Humidity factor
    - Reflectors
    - Photocatalyst
    - External ozone
    - Different types of VOCs

This would mean that the simulation would represent the real reactors even more accurately. Also, it would be possible to change the simulation depending on which type of reactor is wanted and in what environment it is used. Thus, it would both be possible to simulate UV-reactors in many diverse chemical processes.

# 7. REFERENCES


[1] G. E. P. Box, "Robustness in the strategy of scientific model building," *Academic press,* pp. 201-236, 1979.

[2] World Health Organization, "Ambient air pollution: A global assessment of exposure and burden of disease," World Health Organization, Geneva, Switzerland, 2016.

[3] M. Gustafsson, B. Forsberg, H. Orru, S. Åström, H. Tekie and K. Sjöberg, "Quantification of population exposure to NO2, PM2.5 and PM10 and estimated health impacts in Sweden 2010," IVL, Swedish Environmental Research Institute, Göteborg, Sweden, 2014.

[4] J. Fenger, "Urban air quality," *Atmospheric Environment,* vol. 33, pp. 4877-4900, 1999.

[5] K. Chetehouna, Volatile Organic Compounds: Emission, Pollution and Control, Bourges, France: Nova Science Publisher, Inc., 2014.

[6] United States Environmental Protection Agency, EPA Air Pollution Control Cost Manual, North Carolina: US EPA, Office of Air Quality Planning and Standards, 2002.

[7] J. Zhao and X. Yang, "Photocatalytic oxidation for indoor air purification: a litterature review," *Building and Environment,* vol. 38, pp. 645-654, 2003.

[8] G. Busca, S. Berardinelli, C. Resini and L. Arrighi, "Technologies for the removal of phenol from fluid streams: A short review of recent developments," *Journal of Hazardous Materials,* vol. 160, pp. 265-288, 2008.

[9] B. A. Wols, J. A. M. H. Hofman, E. F. Beerendonk, W. S. J. Uijttewaal and J. C. van Dijk, "A Systematic Approach for the Design of UV Reactors Using Computational Fluid Dynamics," *American Institute of Chemical Engineers Journal,* vol. 57, no. 1, pp. 193-207, 2011.

[10] J. Jeong, K. Sekiguchi, W. Lee and K. Sakamoto, "Photodegradation of gaseous volatile organic compounds (VOCs) using TiO2 photoirradiated by an ozone-producing UV lamp: decomposition characteristics, identification of by-products and water-soluble organic intermediates," *Journal of Photochemistry and Photobiology,* vol. A:Chemistry, no. 169, pp. 279-287, 2005.

[11] K.-L. Chang, K. Sekiguchi, Q. Wang and F. Zhao, "Removal of Ethylene and Secondary Organic Aerosols Using UV-C254+185 nm with TiO2 Catalyst," *Aerosol and Air Quality Research,* vol. 13, pp. 618-626, 2013.

[12] The Council of the European Union, "Council directive 1999/13/EC," *Official Journal of the European Communities,* pp. 85/1-85/22, 1999.

[13] R. M. Heck, R. J. Farrauto and S. T. Gulati, Cataytic Air Pollution Contol: Commercial Technology, 3rd Edition, New Jersey: John Wiley & Sons, Inc, 2009.

[14] G. R. Parmar and N. N. Rao, "Emerging Control Technologies for Volatile Organic Compounds," *Critical Reviews in Environmental Science and Technology,* vol. 39, pp. 41-78, 2009.

[15] T. Ioannides, P. Papaefthimiou and X. E. Verykios, "Catalytic incineration of volatile organic compounds present in industrial waste streams," *Applied Thermal Engineering,* vol. 18, pp. 1005-1012, 1998.

[16] G. Busca, S. Berardinelli, C. Resini and L. Arrighi, "Technologies for the removal of phenol from fluid streams: A short review of recent developments," *Journal of Hazardous Materials,* vol. 160, pp. 265-288, 2008.

[17] C. H. Bartholomew and R. J. Farrauto, Fundamentals of industrial catalytic processes, Second Edition, Hoboken, New Jersey: John Wiley & Sons. Inc., 2006.

[18] C. Easter, C. Quigley, P. Burrowes, J. Witherspoon and D. Apgar, "Odor and air emissions control using biotechnology for both collection and wastewater treatment systems," *Chemical Engineering Journal,* vol. 113, pp. 93-104, 2005.

[19] A. Downes and T. P. Blunt, "Research on the Effect of Light upon Bacteria and other Organisms," *Proceedings of the Royal Society of London,* pp. 488-500, 1 January 1877.

[20] G. Porter, "A new method for the study of free radical reactions," *Proceedings of the royal society A,* pp. 284-300, 6 January 1950.

[21] Nobel Media AB, "The Nobel Prize in Chemistry 1967," Nobel Media AB, 2014. [Online]. Available: http://www.nobelprize.org/nobel_prizes/chemistry/laureates/1967/index.html. [Accessed 04 04 2017].

[22] N. Serpone, A. V. Emeline, S. Horikoshi, V. N. Kuznetsov and V. K. Ryabchuk, "On the genesis of heterogeneous photocatalysis: A brief historical perspective in the period 1910 to the mid-1980s," *Photochemical & Photobiological Science,* vol. 11, pp. 1121-1150, 2012.

[23] A. Fujishima and K. Honda, "Electrochemical Photolysis of Water at a Semiconductor Electrode," *Nature,* vol. 238, pp. 37-38, 1972.

[24] S. J. Teichner, "The origins of photocatalysis," *Journal of Porous Materials,* vol. 15, no. 3, pp. 311-314, 2008.

[25] E. R. Blatchley III, "Numerical Modelling of UV Intensity: Application to Collimated-Beam Reactors and Continuous-Flow Systems," *Water Research,* vol. 31, no. 9, pp. 2205-2218, 1997.

[26] J. Jeong, K. Sekiguchi and K. Sakamoto, "Photochemical and photocatalytic degradation of gaseous toluene using short-wavelength UV irradiation with TiO2 catalyst: comparison of three UV sources," *Chemosphere,* vol. 57, pp. 663-671, 2004.

[27] S. Schalk, V. Adam, E. Arnold, K. Brieden, A. Voronov and H.-D. Witzke, "UV-lamps for Disinfection and Advanced Oxidation - Lamp Types, Technologies and Applications," *IUVA News,* vol. 8, no. 1, pp. 32-37, 2006.

[28] Y. Lu, X. Zhao, M. Wang, Z. Yang and X. Zhang, "Feasibility analysis on photocatalytic removal of gaseous ozone in aircraft cabins," *Building and Environment,* vol. 81, pp. 42-50, 2014.

[29] T. Coenen, W. Van de Moortel, F. Logist, J. Luyten and J. F. Van Impe, "Modeling and geometry optimization of photochemical reactors: Single- and multi-lamp reactors for UV-H2O2 AOP systems," *Chemical Engineering Science,* vol. 96, pp. 174-189, 2013.

[30] P. Zhang, F. Liang, G. Yu, Q. Chen and W. Zhu, "A comparative study on decomposition of gaseous toluene by O3/UV, TiO2/UV and O3/TiO2/UV," *Journal of photochemistry and photobiology,* vol. A:Chemistry, no. 156, pp. 189-194, 2003.

[31] K. L. Bell, P. G. Burke, A. Hibbert and A. E. Kingston, "Photoionisation of the 2p4 3P, 1D, 1S states of atomic oxygen," *Journal of Physics B: Atomic, Molecular and Optical Physics,* vol. 22, pp. 3197-3204, 1989.

[32] A. Davydov, K. T. Chuang and A. R. Sanger, "Mechanism of H2S Oxidation by Ferric Oxide and Hydroxide Surfaces," *Journal of Physical Chemistry B,* vol. 102, pp. 4745-4752, 1998.

[33] D. O. Scanlon, C. W. Dunnill, J. Buckeridge, S. A. Shevlin, A. J. Logsdail, S. M. Woodley, R. A. Catlow, M. J. Powell, R. G. Palgrave, I. P. Parkin, G. W. Watson, T. W. Keal, P. Sherwood, A. Walsh and A. A. Sokol, "Band alignment of rutile and anatase TiO2," *Nature Materials,* vol. 12, pp. 798-801, 2013.

[34] J. Schneider, M. Matsuoka, M. Takeuchi, J. Zhang, Y. Horiuchi, M. Anpo and D. W. Bahnemann, "Understanding TiO2 Photocatalyst: Mechanisms and Materials," *Chemical Reviews,* vol. 114, no. Titanium Dioxide Nanomaterials, p. 9919–9986, 2014.

[35] V. S. Priya and L. Philip, "Photocatalytic Degradation of Aqueous VOCs Using N Doped TiO2: Comparison of Photocatalytic Degradation under Visible and Sunlight Irraditation," *International Journal of Environmental Science and Development,* vol. 6, no. 4, pp. 286-291, 2015.

[36] F. Montecchio, H. Persson, K. Engvall, J. Delin and R. Lanza, "Development of a stagnation point flow system to screen and test TiO2-based photocatalysts in air purification applications," *Chemical Engineering Journal,* vol. 306, pp. 734-744, 2016.

[37] J. Cunningham and B. K. Hodnett, "Kinetic Studies of Secondary Alcohol Photo-oxidation on ZnO and TiO2 at 348 K Studied by Gas-chromatographic Analysis," *Journal of Chemical Society, Fraday Transactions 1,* vol. 77, pp. 2777-2801, 1981.

[38] Y. Luo and D. F. Ollis, "Heterogeneous Photocatalytic Oxidation of Trichloroethylene and Toluene Mixtures in Air: Kinetic Promotion and Inhibition, Time-Dependent Catalytic Activity," *Journal of Catalysis,* vol. 163, pp. 1-11, 1996.

[39] A. Voronov, "New Generation of Low Pressure Mercury Lamps for Producing Ozone," *Ozone: Science and Engineering. Ther Journal of the International Ozone Association,* vol. 30, no. 6, pp. 395-397, 2008.

[40] Heraeus, "Amalgam UV lamps for sidinfection and oxidation," Heraeus, 2017. [Online]. Available: https://www.heraeus.com/en/hng/products_and_solutions/uv_lamps_and_systems/uv_amalgam_lamps.aspx. [Accessed 03 04 2017].

[41] J. R. Bolton, "Calculation of Ultraviolet Fluence Rate Distributions in an Annual Reactor: Significance of Refraction and Reflection," *Water Research,* vol. 34, no. 13, pp. 3315-3324, 2000.

[42] The European Parliament and Council, "Directive 2002/3/EC of The European Parliament and the Council Relating to Ozone in Ambient Air," *Official Journal of the European Communities,* pp. 67/14-67/30, 2002.

[43] World Health Organization, "WHO Air quality guidelines for particulate matter, ozone, nitrogen dioxide and sulfur dioxide. Global update 2005. Summary of risk assessment," World Health Organization, Geneva, Switzerland, 2006.

[44] Y. Boyjoo, H. Sun, J. Liu, V. K. Pareek and S. Wang, "A review on photocatalysis for air treatment: From catalyst development," *Chemical Engineering Journal,* vol. 310, pp. 537-559, 2017.

[45] P. Pichat, J. Disdier, C. Hoang-Van, D. Mas, G. Goutailler and C. Gaysse, "Purification/deodorization of indoor air and gaseous effluents by TiO2 photocatalysis," *Catalysis today,* vol. 63, pp. 363-369, 2000.

[46] C. H. Ao, S. C. Lee, C. L. Mak and L. Y. Chan, "Photodegradation of volatile organic compounds (VOCs) and NO for indoor air purification using TiO2: promotion versus inhibition effect of NO," *Applied Catalysis,* vol. B: Environment, no. 42, p. 119–129, 2003.

[47] L. Cao, Z. Gao, S. L. Suib, T. N. Obee, S. O. Hay and J. D. Freihaut, "Photocatalytic Oxidation of Toluene on Nanoscale TiO2 Catalysts: Studies of Deactivation and Regeneration," *Journal of Catalysts,* vol. 196, pp. 253-261, 2000.

[48] H. Valdés, M. Sánchez-Polo, J. Rivera-Utrilla and C. A. Zaror, "Effect of Ozone Treatment on Surface Properties of Activated Carbon," *Langmuir,* vol. 18, pp. 2111-2116, 2002.

[49] Swedish National Infrastructure for Computing, "A description of the hardware, System at a glance," KTH (The Royal Institute of Technology) PDC center for high performance computing, [Online]. Available: https://www.pdc.kth.se/resources/computers/tegner/hardware. [Accessed 15 04 2017].

[50] J. Ducoste and K. Linden, Hydrodynamic Characterization of UV reactors, Denver: Awwa Research Foundation, 2006.

[51] A. Hornbacher, "Steel versus Aluminum. Weight, Strength, Cost, Malleability Comparison," Wenzel Metal Spinning, 2017. [Online]. Available: http://www.wenzelmetalspinning.com/steel-vs-aluminum.html. [Accessed 20 04 2017].

[52] M. T. Suidan and B. F. Severin, "Light Intensity Models for Annular UV Disinfection Reactors," *American Insitute of Chemical Engineers Journal,* vol. 32, no. 11, pp. 1902-1909, 1986.

[53] S. M. Jacob and J. S. Dranoff, "Light Intensity Profiles in a Perfectly Mixed Photoreactor," *American Insitute of Chemical Engineers Journal,* vol. 16, no. 3, pp. 359-363, 1970.

[54] M. H. Kaffash, D. D. Ganji and M. H. Nobakhti, "An analytical solution of turbulent boundary layer fluid flow over a flat plate at high Reynolds number," *Journal of Molecular Liquids,* vol. 230, pp. 625-633, 2017.

[55] W. Frei, "Which Turbulence Model Should I Choose for My CFD Application?," COMSOL®, 16 09 2013. [Online]. Available: https://www.comsol.com/blogs/which-turbulence-model-should-choose-cfd-application/. [Accessed 31 03 2017].

[56] B. E. Launder and D. B. Spalding, "The numerical computation of turbulent flows," *Computer methods in applied mechanics and engineering,* vol. 3, pp. 269-289, 1974.

[57] COMSOL®, "Navier-Stokes equations," COMSOL Inc., 2017. [Online]. Available: https://www.comsol.com/multiphysics/navier-stokes-equations. [Accessed 31 03 2017].

[58] COMSOL®, "Convection-Diffusion Equation," COMSOL Inc., 2017. [Online]. Available: https://www.comsol.com/multiphysics/convection-diffusion-equation. [Accessed 03 04 2017].

[59] COMSOL®, "Fluid Flow, Heat Transfer, and Mass Transport," COMSOL Inc., 2017. [Online]. Available: https://www.comsol.com/multiphysics/fluid-flow-heat-transfer-and-mass-transport. [Accessed 03 04 2017].

[60] M. Zhang, T. An, J. Fu, G. Sheng, X. Wang, X. Hu and X. Ding, "Photocatalytic degradation of mixed gaseous carbonyl compounds at low level on adsorptive TiO2/SiO2 photocatalyst using a fluidized bed reactor," *Chemosphere,* vol. 64, no. 3, pp. 423-431, 2006.

# APPENDIX

## I. Conversion Summaries

Below is a summation of all the conversions calculated for the different simulations, for easy comparison of the cases. The conversions are split up into two, one showing the conversion given by the COMSOL Multiphysics® 5.2a simulations called *Conv.*, while the other is the calculated normalized conversion, called *Norm. conv.* The volume, amount of light sources and sizing parameter for each reactor is also shown.

*Table 8. The volume, number of lamps and fitting parameter $k_{size}$ for every cubical reactor. Together with the conversion obtained from the COMSOL® simulations and the calculated normalized conversion used in the discussion of this thesis.*

| CUBICAL REACTORS | | | | | |
|---|---|---|---|---|---|
| **Case** | **Volume [m³]** | **Number of lamps** | **$k_{size}$** | **Conv.** | **Norm. conv.** |
| **1** | 0.045 | 10 | 1.56 | 20.9% | 100.0% |
| **2** | 0.045 | 10 | 1.56 | 21.4% | 102.1% |
| **3** | 0.045 | 10 | 1.54 | 20.3% | 97.0% |
| **4a** | 0.011 | 11 | 1.76 | 5.1% | 89.3% |
| **4b** | 0.016 | 11 | 1.71 | 8.0% | 96.3% |
| **4c** | 0.029 | 11 | 1.65 | 15.2% | 103.1% |
| **4d** | 0.036 | 11 | 1.63 | 19.3% | 103.4% |
| **4e** | 0.045 | 11 | 1.61 | 23.5% | 101.7% |
| **4f** | 0.065 | 11 | 1.57 | 32.0% | 96.8% |
| **4g** | 0.088 | 11 | 1.54 | 40.7% | 90.2% |
| **4h** | 0.115 | 11 | 1.52 | 49.0% | 83.3% |
| **4i** | 0.145 | 11 | 1.50 | 56.6% | 76.0% |
| **4j** | 0.179 | 11 | 1.49 | 63.7% | 69.2% |
| **5** | 0.045 | 10 | 1.56 | 20.2% | 96.1% |
| **6** | 0.022 | 10 | 1.56 | 9.1% | 87.2% |
| **7** | 0.045 | 3 | 1.49 | 16.0% | 84.8% |
| **8** | 0.031 | 11 | 1.61 | 15.6% | 96.9% |
| **9** | 0.031 | 11 | 1.61 | 13.0% | 80.9% |
| **10a** | 0.045 | 10 | 1.56 | 21.8% | 103.6% |
| **10b** | 0.045 | 10 | 1.56 | 23.3% | 110.7% |
| **11a** | 0.045 | 11 | 1.61 | 25.9% | 112.3% |
| **11b** | 0.045 | 11 | 1.61 | 27.2% | 117.3% |
| **11c** | 0.045 | 11 | 1.61 | 33.7% | 145.1% |

*Table 9. The volume, number of lamps and fitting parameter $k_{size}$ for every cyclone reactor. Together with the conversion obtained from the COMSOL® simulations and the calculated normalized conversion used in the discussion of this thesis.*

| CYCLONE REACTORS | | | | | |
|---|---|---|---|---|---|
| **Case** | **Volume [m³]** | **Number of lamps** | **$k_{size}$** | **Conv.** | **Norm. conv.** |
| **A1** | 0.090 | 12 | 1.42 | 52.6% | 104.1% |
| **A2** | 0.101 | 12 | 1.42 | 56.0% | 99.4% |
| **B1** | 0.065 | 12 | 1.42 | 38.5% | 106.0% |
| **B2** | 0.073 | 12 | 1.42 | 43.2% | 105.2% |
| **C** | 0.051 | 12 | 1.61 | 38.0% | 132.9% |
| **D** | 0.082 | 12 | 1.42 | 50.8% | 110.7% |
| **E** | 0.055 | 12 | 1.42 | 36.2% | 117.5% |
| **F1** | 0.051 | 12 | 1.61 | 34.2% | 119.8% |
| **F2** | 0.051 | 12 | 1.61 | 34.0% | 119.0% |
| **G** | 0.095 | 9 | 1.38 | 34.8% | 87.6% |
| **H** | 0.167 | 12 | 1.22 | 64.0% | 68.3% |
| **I** | 0.095 | 12 | 1.38 | 49.9% | 94.2% |
| **J** | 0.095 | 12 | 1.46 | 57.4% | 107.8% |
| **K** | 0.051 | 12 | 1.61 | 38.7% | 135.5% |
| **L** | 0.051 | 12 | 1.79 | 46.0% | 161.0% |
| **M** | 0.051 | 12 | 1.87 | 44.3% | 155.3% |

## II. Trademarks

ANSYS, FLUENT and any and all ANSYS, Inc. brand, product, service and feature names, logos and slogans are registered trademarks or trademarks of ANSYS, Inc. or its subsidiaries in the United States or other countries. All other brand, product, service and feature names or trademarks are the property of their respective owners.

COMSOL and COMSOL Multiphysics are registered trademarks of COMSOL AB.

MATLAB is a registered trademark of The MathWorks, Inc.